



# Hepatoprotective and neuroprotective effects of quinacrine against bile duct ligation-induced hepatic encephalopathy in rats: Role of bone morphogenetic proteins signaling

Manar M. Esmail<sup>a</sup>, Noha M. Saeed<sup>a</sup>, Diana M.F. Hanna<sup>b</sup>, Haidy E. Michel<sup>b</sup>, Reem N. El-Naga<sup>b</sup>, Samar S. Azab<sup>b,\*</sup>

<sup>a</sup> Department of Pharmacology and Toxicology, Faculty of Pharmacy, Egyptian Russian University, Cairo, Egypt

<sup>b</sup> Department of Pharmacology and Toxicology, Faculty of Pharmacy, Ain Shams University, Cairo, Egypt

## ARTICLE INFO

**Keywords:**

Bile duct ligation  
Bone morphogenetic proteins  
Farnesoid x receptor  
Hepatic encephalopathy  
Quinacrine  
WNT pathway

## ABSTRACT

**Aims:** This study aimed to assess the potential protective effect of quinacrine, an FDA approved antimalarial drug with reported anti-inflammatory effects, on hepatic encephalopathy (HE) in a bile duct ligation (BDL) experimental model and to investigate the mechanisms responsible for this effect, namely those associated with the liver-brain axis, particularly, bone morphogenetic protein 2 (BMP2) signaling.

**Materials and methods:** Five groups of rats were selected at random: sham, BDL, (BDL+ quinacrine 5), (BDL+ quinacrine 10), and (quinacrine 10 + sham). Daily Intraperitoneal (I.P.) administration of quinacrine was initiated on the surgery day and continued for 28 days.

**Key findings:** Results showed that rats that underwent BDL exhibited marked elevation of serum liver enzymes, ammonia, total bilirubin, together with oxidative stress, inflammation, dysregulated farnesoid x receptor (FXR), dysregulated BMP2 signaling and escalated fibrotic markers indicating hepatotoxicity, cholestasis and fibrosis. Besides, neurotoxicity was detected as manifested by cognitive deficits and dysregulation of hippocampal FXR, BMP2 signaling, WNT3A signaling, brain derived neurotrophic factor (BDNF), phospholipase A2 (PLA2) and glial fibrillary acidic protein (GFAP). In contrast, co-treatment with quinacrine mitigated BDL-induced hepatotoxicity, cholestasis, fibrosis, and neurotoxicity. Notably, quinacrine improved learning and memory and restored FXR, BMP2 signaling in the liver and hippocampus. In addition, quinacrine restored hippocampal WNT3A signaling, BDNF, whereas it downregulated expression of hippocampal PLA2 and GFAP.

**Significance:** These findings demonstrated implication of BMP2 signaling in the molecular process of BDL-induced HE and proposed that quinacrine has potential hepatoprotective and neuroprotective properties against HE.

## 1. Introduction

Hepatic encephalopathy (HE) is a neurological condition linked to both acute and chronic liver diseases. This illness can result in a variety of cognitive and physical disabilities, alterations in personality, difficulties with focus, and disruptions in sleep patterns and reduced levels of consciousness that may eventually progress to coma and death [1].

The development of HE is primarily attributed to the significant contribution of hyperammonemia and inflammation, which act in a synergistic manner [2]. Abnormal amounts of ammonia in the brain due to a malfunctioning urea cycle leads to disturbances in intracellular pH and cellular metabolism. These anomalies contribute to a cascade of

subsequent neurological consequences and the development of encephalopathy [3]. Experimental models of liver failure have been reported to show an elevation in peripheral pro-inflammatory cytokines, such as tumor necrosis factor- $\alpha$  (TNF- $\alpha$ ), and interleukin-6 (IL-6) [4]. These pro-inflammatory mediators can trigger and activate astrocytes and microglia via three routes: the neural pathway by activating the vagal afferent in the liver, the blood brain barrier (BBB) endothelial cells pathway and circumventricular organs (regions in brain that lack intact BBB) pathway leading to cerebral inflammation and HE [5,6].

Other pathogenic factors, including oxidative stress and elevated levels of bile acids, may act in conjunction with hyperammonemia and inflammation to exacerbate the development of HE [3]. In addition,

\* Corresponding author at: Pharmacology and Toxicology Department, Faculty of Pharmacy, Ain Shams University, Cairo 11566, Egypt.

E-mail address: [samar\\_saad\\_azab@pharma.asu.edu.eg](mailto:samar_saad_azab@pharma.asu.edu.eg) (S.S. Azab).

bone morphogenetic proteins (BMPs), which are growth factors classified under the transforming growth factor- $\beta$  (TGF- $\beta$ ) category, were initially discovered as factors involved in bone formation [7]. However, recent studies have highlighted the neuroprotective and antifibrotic effects of these proteins. It is well-known that TGF- $\beta$ 1 is vital in fibrogenesis within the liver. It has been found that BMP2 can effectively counteract the fibrotic effects of TGF- $\beta$ 1, thereby mitigating the progression of fibrosis [8]. In the brain, BMP signaling pathway is vital in regulating the process of adult neurogenesis and neuronal survival. [9,10]. Furthermore, BMP works in close collaboration with the WNT signaling pathway [9] which has a role in mitigating neuroinflammation and oxidative stress effects [11].

Quinacrine is an FDA-approved antimalarial drug that has been identified as a potent inhibitor of phospholipase A2 (PLA2) [12]. It is acknowledged for its ability to reduce oxidative stress and inflammation [12–14]. Recent findings suggest that quinacrine triggers BMP-Smad-dependent transcription, resulting in a significant elevation in P-Smad -1/5/8 levels in neurons [15].

Bile duct ligation (BDL) is a widely recognized method which reliably promotes cirrhosis in rats. The International Society for Hepatic Encephalopathy and Nitrogen Metabolism has recognized this model as being among the few models that faithfully replicate the features of, HE results from liver diseases [6,16]. Accordingly, this study aimed to investigate the potential protective role of quinacrine in HE via using BDL experimental model and explore the underlying mechanisms, namely those associated with the liver-brain axis, particularly, BMP2 signaling.

## 2. Materials and methods

### 2.1. Chemicals

Quinacrine dihydrochloride and ketamine were acquired from Sigma-Aldrich, MO, USA (Catalogue No. Q3251 and Catalogue No. 2753, respectively). The selection of quinacrine doses was based on the findings from earlier trials [12,17,18].

### 2.2. Animals

Male Wistar rats, 12 weeks old, 200–250 g, were acquired from Nile Co., a company specializing in pharmaceutical and chemical industries based in Cairo, Egypt. The Ain Shams University Research Ethics Committee (ACUC-FP-ASU RHDIRB2020110301REC#106) in Egypt approved all experimental techniques, including those involving animals, and ensured compliance with their regulations. Prior to commencing the experiment, the rats were given a one-week period to acclimate. Throughout this duration, the subjects were subjected to typical circumstances, including a light/dark cycle of 12 h each, and were maintained at a temperature ranging from 22 to 24 °C. The rats were given free and unfettered availability of food and water.

### 2.3. The experimental design

A total of sixty rats were allocated into five groups, with each group consisting of twelve rats, using a random assignment method. Group 1 (sham) comprised of rats that received a sham operation. Group 2 (BDL) comprised of rats that underwent BDL. Group 3 (BDL/quinacrine 5) consisted of rats that underwent BDL followed by intraperitoneal (i.p.) administration of quinacrine (5 mg/kg/day) for 28 days. Group 4 (BDL/quinacrine 10) consisted of rats that received BDL, thereafter quinacrine was injected i.p. (10 mg/kg/day) for 28 days. Group 5 (quinacrine 10/sham) consisted of rats that received a sham operation, thereafter quinacrine was injected i.p. (10 mg/kg/day) for 28 days. Quinacrine was dissolved in distilled water (freshly prepared) and injections began on the same day as the surgery. A priori power analysis was performed utilizing G\*Power (version 3.1.9.7, Heinrich-Heine University,

Germany) to determine the requisite total sample size for the proposed experimental model. The analysis was conducted with an alpha error of 0.05, a power level of 0.85, and an effect size of 0.5. A total sample size of 60 animals (12 each group) was established based on these criteria. The experimental design is illustrated in (Fig. 1).

### 2.4. BDL operation

Ketamine (90 mg/kg/i.p.) was used to put the rats under anesthesia [19]. To ligate the bile duct, two surgical knots were employed in conjunction with 4–0 silk sutures following the protocol described in [20,21]. For the sham group, a laparotomy (Bile duct isolation without ligation) was performed instead of ligation. The rats were then placed under a warm source of heat, an infrared lamp, until they regained consciousness and became active.

### 2.5. Behavioral tests

At the completion of the experiment on day 28, the animals underwent behavioral assessments on day 29 and day 30.

#### 2.5.1. Open field test

The open field (OF) test was carried out on day 30 to assess the possible impact of BDL and quinacrine therapy on locomotion and anxiety-like behaviors. The square wooden box that served as the testing apparatus had red walls and a polished black floor, and its dimensions were 80 × 80 × 40 (H) cm. White lines were used to divide the box into sixteen equal squares. Every rat was positioned in middle of the enclosure then given a five-minute opportunity to investigate the surroundings. A camera mounted above the rats recorded their ambulation frequency, which refers to the number of squares that each rat traveled, rearing frequency, which refers to the number of times that their hind limbs were raised, and total time spent in the center. Floor was cleaned with cotton cloth after each animal was tested [22,23].

#### 2.5.2. Morris water maze

The Morris water maze (MWM) test was employed to evaluate spatial learning and memory. The rats were subjected to training to navigate towards a circular platform located in a pool with inner surfaces that do not reflect light. The pool was 60 cm tall and 150 cm in diameter, divided into four equal sections and filled with water up to a depth of 35 cm. A 9-cm-diameter movable circular platform was placed in the exact middle of one of the four corners, only one centimeter below the water's surface, for the purpose of conducting the acquisition test. The pool water was dyed black using harmless soluble paint. The rats participated in three daily training sessions, each lasting 120 s, for a duration of four days (from day 25 to 28). During the training sessions, from a variety of beginning points, the rats were allowed to explore their surroundings and find the platform. Quantification of the acquisition latency was accomplished by determining the average amount of time the rat took to arrive to the platform. During the fifth day, which was day 29, a probing test was carried out. The platform was eliminated, and the rat was set free, positioned towards the pool wall in the quadrant that across from the target quarter. An overhead camera was employed to capture the whole duration of the rat's swimming activity in the targeted quadrant, following a two-minute period of pool exploration [24,25].

#### 2.5.3. Novel object recognition

A novel object recognition (NOR) test was carried out to assess cognitive abilities, specifically the ability to remember and recognize objects. The experiment took place in a black rectangular field enclosure that was 50 cm long, 25 cm wide, and 50 cm high. During habituation phase, which took place on day 26 and 27, The rats were given unrestricted access to the test box without any objects for a duration of ten min per day, over the two days. During the training phase on day 28, two identical objects were placed in each corner of the test box, about 30 cm

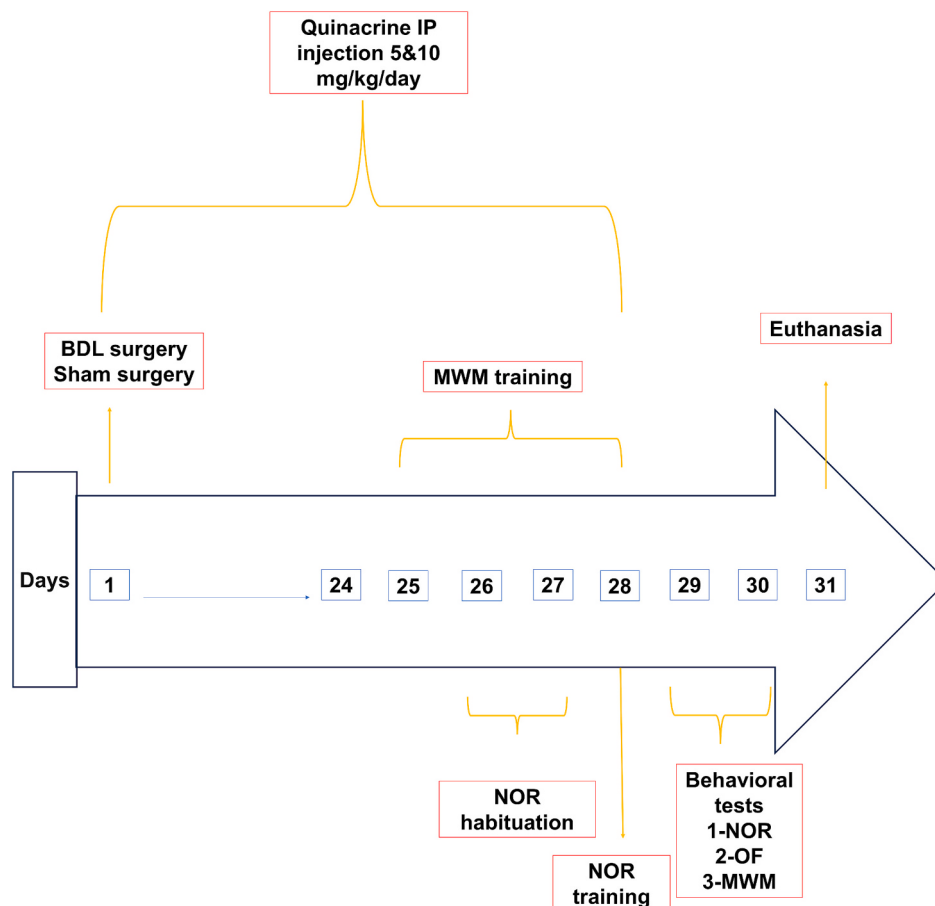


**Fig. 1.** Timeline of the experimental model.

apart and each rat was then placed in the box and allowed to explore for a duration of 5 min. On the 29th day (test day), the animals were reintroduced inside the test box, to which a new object was added in place of one of the objects that they had previously been familiar with. Rats were allotted for a duration of 3 min to investigate the objects, and the duration of exploration for each object was documented using the overhead camera. The cumulative duration of investigating both the known and unfamiliar objects was computed. In addition, the discriminating index was computed as the difference in the amount of time consumed examining familiar and novel things, divided by the overall exploration time of both objects [26].

## 2.6. Study termination

Following the end of the behavioral testing, the rats underwent an overnight fast. On the 31st day, blood samples were obtained from the retro-orbital plexus and subjected to centrifugation to isolate the serum. The serum was then divided into aliquots and preserved at a temperature of  $-80^{\circ}\text{C}$  until further examination. Following the collection of blood, the rats were euthanized via cervical dislocation. The liver and brain tissues were promptly extracted, cleaned, and dissected. For subsequent examinations, hippocampi were dissected from brain tissues, then hippocampal as well as liver tissues of each sample were submerged in liquid nitrogen and thereafter preserved at  $-80^{\circ}\text{C}$ . For histological examination, whole brains as well as liver tissues of each sample of the tissues were preserved in a solution of 10 % neutral buffered formalin.

## 2.7. Colorimetric assay for

### 2.7.1. Hepatotoxicity markers

Using a colorimetric assay, the serum levels of aspartate transaminase (AST) and alanine transaminase (ALT) were determined following the instructions provided by TECO DIAGNOSTICS in Anaheim, CA, USA (catalogue No. A561 and A526, respectively). The AST and ALT results were reported in (U/L).

### 2.7.2. Cholestasis markers

A colorimetric test was performed with a commercial kit (catalogue No. 5601-01 Gateway Dr. W Thurmont, Maryland) in order to quantify the levels of serum gamma-glutamyl transferase (GGT). Serum alkaline phosphatase (ALP) concentration was ascertained by use of a colorimetric assay following the manufacturer-specified protocols, provided by BioAssay Systems in Hayward, CA, USA, at 3191 Corporate Place 94,545 (catalogue No. A526). Values of GGT and ALP were expressed as U/L.

The concentration of serum total ammonia and total bilirubin were quantified using commercially available colorimetric assay kits (Abcam, Waltham, MA, USA, catalogue No. ab83360 and catalogue No. ab235627), respectively. Values were expressed as mmol/ml and mg/100 ml, respectively.

### 2.7.3. Protein assay in tissue homogenates

The concentration in the tissue homogenate was evaluated using the Bradford procedure, as outlined in the Bradford assay kit, Abcam, Waltham, USA, (catalogue No. ab102535).

## 2.8. Enzyme-linked immunosorbent assay (ELISA) for:

### 2.8.1. Assessment of oxidative stress markers

The levels of malondialdehyde (MDA) and reduced glutathione (GSH) in the liver and hippocampus were assessed using the instructions provided by the manufacturer for Catalogue No. MBS268427 from MyBioSource in SD, USA and catalogue No. E02G0367 from blue gene Biotech CO., in China, respectively. The results of the experiments were reported in units of (nmol/mg protein) and (pg/mg protein), respectively. The liver tissue levels of superoxide dismutase (SOD) were assessed following the guidelines provided by the manufacturer (catalogue No. MBS036924 from MyBioSource in SD, USA). The values of Superoxide Dismutase (SOD) were quantified and reported as (U/mg protein).

### 2.8.2. Assessment of inflammatory markers

The IL-6 and TNF- $\alpha$  levels in the serum were determined by ELISA kits from MyBioSource in SD, USA (Catalogue No. MBS2021530 and catalogue No. MBS824824, respectively). The ELISA procedure involved several steps: first, serum samples were prepared and diluted as per the manufacturer's instructions, followed by coating the wells of the ELISA plates with the samples and incubating them overnight at 4 °C. After washing the wells to remove unbound substances, enzyme-conjugated antibodies specific to IL-6 and TNF- $\alpha$  were added, and the plates were incubated again. A substrate solution was then introduced to produce a colour change proportional to the concentration of the target proteins, which were measured using a microplate reader. The concentrations of IL-6 and TNF- $\alpha$  were reported in (pg/ml). Additionally, nuclear factor-kappa B (NF- $\kappa$ B) levels in liver tissue were assessed using the NF- $\kappa$ B ELISA kit (Catalogue No. MBS453975 from My BioSource in SD, USA). The NF- $\kappa$ B assay followed a similar procedure, with results normalized to total protein content and expressed in (ng/mg protein).

### 2.8.3. Determination of hydroxyproline content

The hydroxyproline content in tissue samples was evaluated using an ELISA kit from MyBioSource (Catalogue No. MBS017427), following the detailed protocols provided by the manufacturer. The procedure began with the preparation of tissue samples, which were then diluted as necessary. The wells of the ELISA plates were subsequently coated with the diluted samples and incubated. After a thorough washing step, enzyme-conjugated antibodies specific to hydroxyproline were introduced, followed by another incubation period to allow for effective binding. The addition of a substrate solution then triggered a colorimetric reaction, which was measured using a microplate reader for quantification. To ensure accuracy and consistency, the hydroxyproline levels were normalized against the total protein content and expressed in ng/mg protein.

## 2.9. Western blot analysis

Western blot technique was used for assessment of the expression of BMP2, P-Smad 1/5/8 and farnesoid X (FXR) proteins in liver and hippocampal tissues and assessment of WNT3A,  $\beta$ -catenin, lymphoid enhancer-binding factor (Lef1), BDNF and PLA2 proteins in hippocampal tissues. Liver and hippocampal tissues' lysates were prepared utilizing RIPA lysis buffer, sourced from Bio BASIC located in Markham, Canada. Subsequently, the lysates were stirred using ice for a duration of 30 min and spun in a centrifuge at 4 °C for 30 min at a force of over 16,000 times gravity in order to eliminate cellular waste. To further determine the protein concentration, the supernatants were transferred to a fresh tube and tested with the Bradford Protein Assay Kit (SK3041) from BIO BASIC INC, Canada. The process of electrophoretic resolution involved loading 20  $\mu$ g of protein onto a 10 % SDS polyacrylamide gel and subsequently transferring it to a polyvinylidene fluoride (PVDF) membrane. A mixture of 3 % bovine serum albumin (BSA) and tris-buffered saline with Tween 20 (TBST) buffer was used to block the

membrane. To prevent non-specific antibody binding, the membranes were left to incubate at an ambient temperature for a duration of 1 h in a Tris buffer solution (pH 7.5) with Tween 20 (0.1 %), 150 mM NaCl and BSA (3 %) (pH 7.5). The following primary antibodies were used: (FXR antibody, Catalogue No. 252165, Suite I Escondido, CA 92029, USA); (BMP2 antibody, Catalogue No. PA5-85956, ThermoFisher in Massachusetts, USA); (P-Smad 1/5/8 Antibody, Catalogue No. AB3848I Sigma-Aldrich, St Louis, USA); (total (T)- Smad 1/5/8 Antibody, Catalogue No. 21684, Signalway Antibody, Maryland, USA) and ( $\beta$  actin antibody, Catalogue No. PA1-183, ThermoFisher in Massachusetts, USA). (WNT3A antibody, Catalogue No. PA5-102317, ThermoFisher in Massachusetts, USA); ( $\beta$ -catenin antibody, Catalogue No. PA5-16762, ThermoFisher in Massachusetts, USA); (Lef1 antibody, Catalogue No. PA5-102851, ThermoFisher in Massachusetts, USA); (brain derived neurotrophic factor (BDNF) antibody, Catalogue No. PA5-85730, ThermoFisher in Massachusetts, USA) and (PLA2 antibody, Catalogue No. PA5-118887, ThermoFisher in Massachusetts, USA). The primary antibodies were diluted in TBST and treated with membranes overnight. After that, the secondary antibody (Goat anti-rabbit secondary antibody, Catalogue No. 65-6120, ThermoFisher in Massachusetts, USA) was incubated at an ambient temperature for a duration of 1 h. Subsequently, for imaging and quantitative data analysis, the blot underwent exposure to the chemiluminescent substrate (ClarityTM ECL substrate - Catalogue No. 170-5060, BIO-RAD, USA). The resulting chemiluminescent signals were captured using a CCD imager. ImageJ software (version 1.50i) was employed to analyze and measure the band intensities of the target proteins in comparison to the control sample following normalization by beta-actin, as previously described [27].

## 2.10. Histopathological examination

After dissecting the liver and brain samples, they were submerged in 10 % neutral buffered formalin for a period of 72 h to fix them. The samples underwent sequential processing in various concentrations of ethanol, followed by treatment with xylene to remove impurities, and finally were immersed in paraplast tissue embedding solution for preservation. Brain sagittal tissue sections, as well as liver tissue sections, with a thickness of 4  $\mu$ m, were sliced by using a rotating microtome and then set on microscope slides. The tissue sections underwent hematoxylin and eosin staining, then liver sections examined under microscope as well as, brain section examined to demonstrate the hippocampal regions. In addition, the liver sections were subjected to staining using Masson's trichrome to see collagen fibers. The previously specified standard techniques for sample fixation and staining were implemented [28]. An expert histopathologist who was blinded to the animal treatments used a Leica application program for tissue section analysis and a full HD microscopic imaging system (Leica Microsystems GmbH, Germany) to acquire the data.

## 2.11. Immunohistochemical analysis for hepatic TGF- $\beta$ 1, $\alpha$ -SMA and hippocampal GFAP

The liver and brain tissue sections, which were 4- $\mu$ m thick and had been deparaffinized, were subjected to treatment with 3 % H2O2 for 20 min in compliance with the guidelines provided by the manufacturer. After being washed, liver sections were then incubated with anti TGF- $\beta$ 1 antibody (NBP2-22114) from NOVUS Bio at a dilution of 1:100, as well as with anti-alpha-smooth muscle actin ( $\alpha$ -SMA) rabbit polyclonal antibody (Abcam, Ab5694) also at a dilution of 1:100. While brain sections were exposed to the anti-glial fibrillary acidic protein antibody (GFAP) (Catalogue No13-0300, Thermo Scientific Co.) at a dilution of 1:100 and left to incubate at 4 °C for the night. Subsequently, the samples underwent washing using phosphate buffered saline (PBS) and were subsequently exposed to horseradish peroxidase (HRP) conjugated secondary antibody, specifically the envision kit (DAKO) for a duration of 20 min. Subsequently, tissue sections were cleansed with PBS and

then exposed to diaminobenzidine (DAB) for a period of ten minutes. After that, there was yet another round of washing using PBS. Following that, the sections underwent hematoxylin staining, drying, and xylene treatment to remove any remaining liquid. Finally, the sections were covered with a slip for viewing under a microscope. Six random non overlapping microscopic fields (images) were randomly picked and analyzed in every tissue sample to quantify for the area percentage of immunohistochemical expression levels of TGF- $\beta$ 1 and  $\alpha$ -SMA in immunostained liver sections and hippocampal GFAP expression levels in brain tissue sections. An expert histopathologist who was blinded to the animal treatments used a Leica application program for tissue section analysis and a full HD microscopic imaging system (Leica

Microsystems GmbH, Germany) to acquire the data [29].

## 2.12. Statistical analysis

The data were reported in the format of mean  $\pm$  standard deviation (SD). The parametric data was analyzed using one-way analysis of variance (ANOVA) followed by Tukey's post-hoc test. The Kruskal-Wallis test, followed by Dunn's multiple comparison test, was utilized to analyze non-parametric data, namely the ambulation frequency and rearing frequency. The significance of variations in familiar and new item exploration time for each group and the analysis of escape latency in the MWM test were determined using two-way ANOVA. A *p*-value

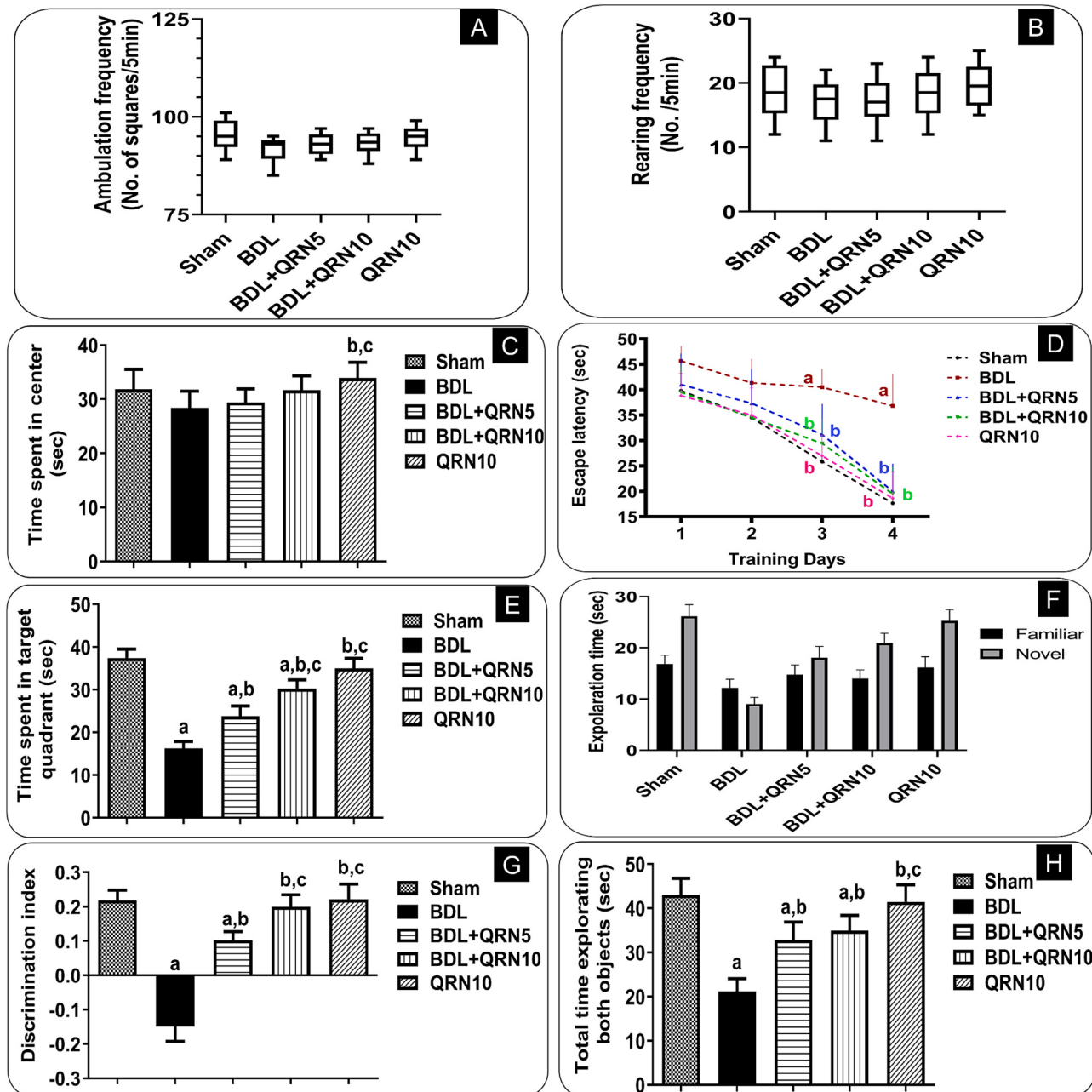


**Fig. 2.** Effects of quinacrine (QRN) on BDL-induced changes in (A) ambulation frequency, (B) rearing frequency, (C) time spent in center in OF test, (D) escape latency, (E) time spent in target quadrant in MWM test, (F) the exploration time of familiar and novel objects, (G) discrimination index and (H) total time exploring both objects in NOR test. Rearing and ambulation frequency are displayed as boxplots with median, 25th and 75th percentile values. These values were obtained using the Kruskal-Wallis test, followed by Dunn's post-hoc test. The parametric data are displayed as the mean  $\pm$  SD of 12 rats per group, with a significance level of *p* < 0.05. This analysis was conducted using a one-way ANOVA followed by Tukey's post-hoc test. Escape latency and differences in familiar and novel object exploration time for each group were assessed by employing two-way ANOVA. a: vs. sham group, b: vs. BDL group, c: vs. (BDL+QRN5) group.

below 0.05 was deemed to be statistically significant. The statistical analysis and charting were performed using version 8 of GraphPad Prism software developed by ISI Software in the United States.

### 3. Results

#### 3.1. The impact of quinacrine on locomotor activity and anxiety (open field test) in BDL rats

In the BDL model, neither general activity levels nor anxiety were found to change. In terms of overall locomotor activity (ambulation frequency), anxiety level (time spent in the center), and rearing frequency, no statistically significant difference was seen among the five groups ( $p > 0.05$ ; depicted in Fig. 2A, B, and C, respectively).

#### 3.2. The impact of quinacrine on spatial learning and memory (Morris water maze task) in BDL rats

Two measurements were taken: the escape latency during the 4-day training period (days from 25 to 28) and the duration of each rat's presence in the targeted region during the 2-min probe experiment. Concerning the duration of escape latency, rats receiving BDL spent significantly more time 1.6- and 2-fold longer, respectively, on comparing to the sham group during the third and fourth days. In contrast, in (BDL + quinacrine 5) and (BDL + quinacrine 10) treated groups, quinacrine resulted in a considerable reduction of the escape latency by 23 % and 45.7 %, respectively, opposed to the BDL group. Co-administering quinacrine at dosage 10 mg/kg led to notable reduction in escape latency by 27.4 % and 47 %, respectively. There was no noticeable distinction observed in the escape latency between the two doses of quinacrine (Fig. 2D).

During the probing trial, the BDL group spent 56.57 % less time in the desired quadrant than the sham group. The target quadrant time was 1.46- and 1.86-fold longer in the (BDL + quinacrine 5) and (BDL + quinacrine 10) treated groups, respectively, compared to the BDL group. Furthermore, a significant difference existed between the two dosages; quinacrine (10 mg/kg) markedly extended the duration in the target quadrant by 1.27-fold compared to (BDL + quinacrine 5) (Fig. 2E).

#### 3.3. The impact of quinacrine on recognition memory (novel object recognition) in BDL rats

In the BDL group, the rats' exploration period of the novel object was substantially shorter than that of the familiar object (26.4 %, Fig. 2F) in the same group and a shorter amount of time spent examining the novel object (65.6 %, Fig. 2F), in comparison to the amount examining the sham group's new item. On the other hand, (BDL + quinacrine 5) group showed a substantial increase in the amount of time investigating the novel object as opposed to the familiar object (1.23-fold, Fig. 2F) in the same group and the duration spent investigating the novel item relative to the novel item of the BDL group (2-fold, Fig. 2F). On the other hand, (BDL + quinacrine 10) group showed a substantial increase in duration spent investigating the novel item than familiar object (1.49-fold, Fig. 2F) in the same group and the duration spent investigating the novel item opposed to the novel object of the BDL group (2.32-fold, Fig. 2F).

Also, BDL rats showed a notable decrease in the discriminating index (Fig. 2G) as well as the overall duration of exploration for both objects (50.77 %, Fig. 2H), opposed to the sham group relative to the BDL group, (BDL + quinacrine 5) group demonstrated a notable improvement in both the discrimination index (shown in Fig. 2G) and the total amount of time investigating both items (1.55-fold shown in Fig. 2H). In addition, (BDL + quinacrine 10) group exhibited a notable enhancement in the discrimination index (Fig. 2G) and the total duration investigating both items (1.65-fold increase, Fig. 2H), relative to the BDL group. Additionally, a notable disparity was observed between the two doses of quinacrine, with the (10 mg/kg) dose in the (BDL + quinacrine 10)

group exhibiting a substantial increase of 1.2-fold in the duration investigating the new item alone (Fig. 2F), along with a higher discrimination index compared to the (5 mg/kg) dose in the (BDL + quinacrine 5) group (Fig. 2G).

#### 3.4. The impact of quinacrine on hepatotoxicity and cholestasis markers

The AST (Fig. 3A), ALT (Fig. 3B), ALP (Fig. 3C), GGT (Fig. 3D), ammonia (Fig. 3E), and total bilirubin (Fig. 3F) levels in BDL group exhibited a substantial rise relative to the sham group. The increase was 4.4-fold for AST, 5.4-fold for ALT, 4-fold for ALP, 7-fold for GGT, 2.6-fold for ammonia, and 3.4-fold for total bilirubin. In contrast, (BDL + quinacrine 5) and (BDL + quinacrine 10) treated groups, quinacrine resulted in substantial reductions. The reductions were as follows: AST (42.37 %, 63.17 %), ALT (53 %, 68.23 %), ALP (41.23 %, 61.9 %), GGT (47.7 %, 75 %), ammonia (27.56 %, 52.24 %), and total bilirubin (41.6 %, 62.73 %). These reductions were observed as compared to the BDL group. In addition, (BDL + quinacrine 10) resulted in a considerable reduction of AST, ALT, ALP, GGT, ammonia, and total bilirubin levels by 36 %, 32.5 %, 35.18 %, 52.3 %, 34.07 %, and 36.17 %, respectively, compared to (BDL + quinacrine 5).

#### 3.5. The impact of quinacrine on the levels of oxidative stress and antioxidant ability

The BDL group showed significantly higher levels of MDA in the liver (Fig. 4A) and hippocampus (Fig. 4B) relative to the sham group; the former showed a 6-fold increase and the latter a 2-fold elevation. Following the administration of quinacrine in the (BDL + quinacrine 5) group, a substantial decrease of 44.77 % and 20.56 %, respectively, was observed in the BDL group. However, when quinacrine was administered (BDL + quinacrine 10) group, it led to a considerable low of MDA levels (68.88 % and 40.42 %) relative to the BDL group. In addition, a considerable low of hepatic and hippocampus levels by 43.66 % and 19.86 % respectively, was observed in the (BDL + quinacrine 10) group relative to (BDL + quinacrine 5) group.

Furthermore, in addition, BDL caused a notable decrease in liver (Fig. 4C) and hippocampal (Fig. 4D) GSH levels, decreasing them by 81 % and 74.28 % respectively, opposed to the sham rats. Conversely, co-administration of quinacrine in the (BDL + quinacrine 5) group substantially raised GSH levels (2.5-fold, 2-fold) in the liver and hippocampus, respectively, contrasted to the BDL group. Co-administration of quinacrine in the (BDL + quinacrine 10) group considerably increased liver and hippocampal GSH levels (4.2-fold, 3-fold), respectively, contrasted to BDL group. In the (BDL + quinacrine 10) group, there was an increase in the liver and hippocampal GSH levels of 1.7- and 1.3-fold respectively, when compared to the (BDL + quinacrine 5) group.

The BDL group exhibited a substantial reduction of 78.33 % in liver SOD levels (Fig. 4E), relative to the sham group. Nevertheless, when quinacrine was administered in the (BDL + quinacrine 5) and (BDL + quinacrine 10) groups, SOD levels increased by 2- and 3-fold respectively, compared to the BDL group. Notably, administering quinacrine (BDL + quinacrine 10) group led to a 1.5-fold rise in SOD levels opposed to (BDL + quinacrine 5) group.

#### 3.6. The impact of quinacrine on inflammatory markers

The levels of IL-6 (Fig. 4F), TNF- $\alpha$  (Fig. 4G), and NF- $\kappa$ B (Fig. 4H) were substantially greater in the BDL group contrasted to sham group, increasing by 5-, 4.7-, and 6-fold, respectively. Nevertheless, quinacrine in the (BDL + quinacrine 5) group resulted in a notable reduction of 37.2 %, 38.12 %, and 46.2 % in these levels, in relation to the BDL group. In addition, administration of quinacrine dose of 10 mg/kg in the (BDL + quinacrine 10) group exulted in a considerable decrease in IL-6, TNF- $\alpha$ , and NF- $\kappa$ B levels relative to the BDL group. Specifically, IL-6 levels were lowered by 57.45 %, TNF- $\alpha$  levels by 58.82 %, and NF- $\kappa$ B levels by

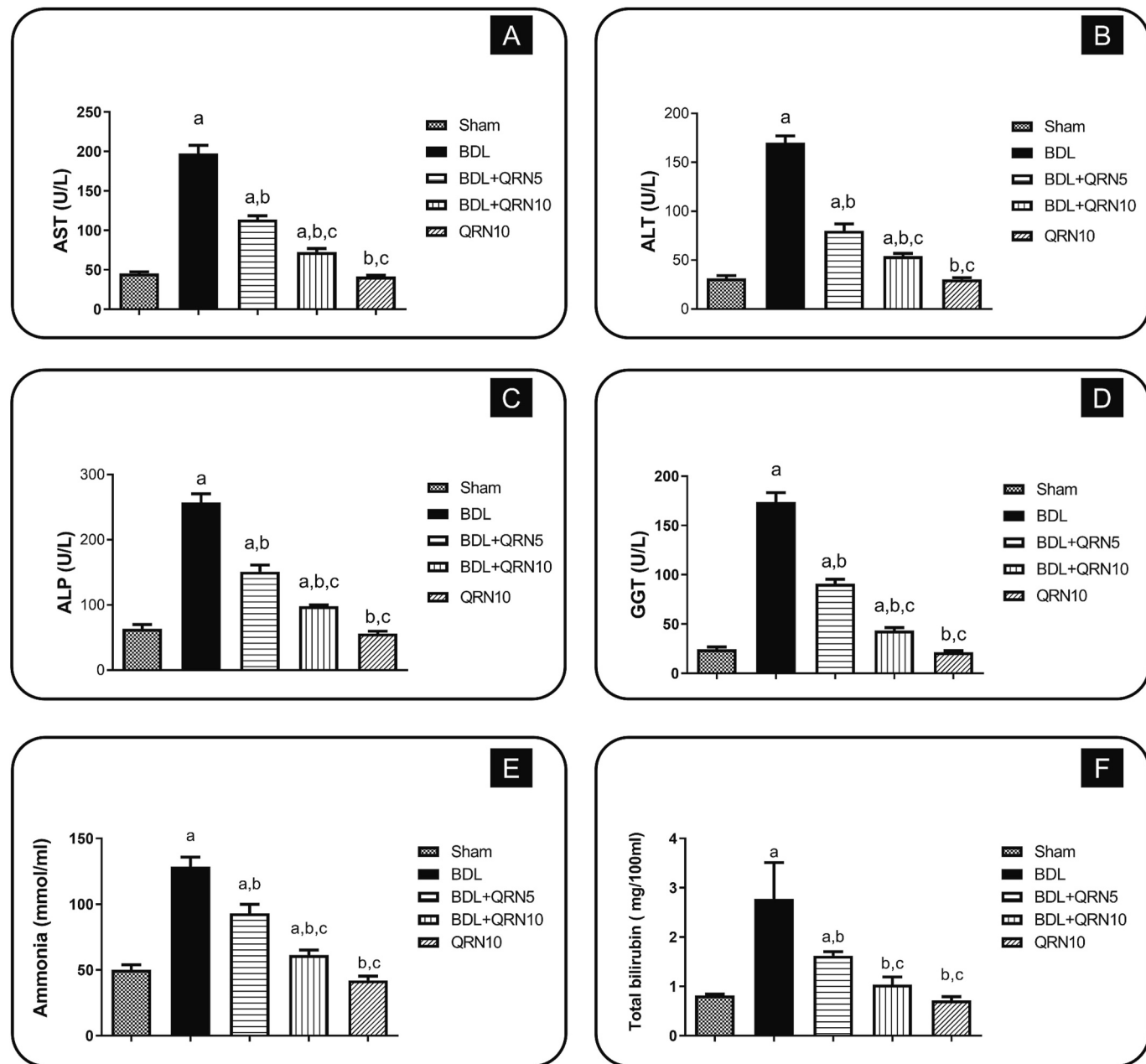


**Fig. 3.** The impact of quinacrine (QRN) on the hepatotoxicity and cholestasis markers in the BDL-induced HE. Serum (A) AST, (B) ALT, (C) ALP, (D) GGT, (E) Ammonia and (F) Total bilirubin. Data are displayed as mean  $\pm$  SD ( $n = 6$ ). a: vs. sham group, b: vs. BDL group, c: vs. (BDL+QRN5) group at  $p < 0.05$  utilizing one-way ANOVA with Tukey's test as the post-hoc analysis.

71.2 %. In addition, in the (BDL + quinacrine 10) group, a notable reduction was showed in IL-6, TNF- $\alpha$ , and NF- $\kappa$ B levels by 32.26 %, 33.46 %, and 46.47 %, respectively, as opposed to the (BDL + quinacrine 5) group.

### 3.7. The impact of quinacrine on liver and hippocampal farnesoid x receptor (FXR)

As presented in Fig. 5, BDL caused a marked reduction in liver (Fig. 5A,B) and hippocampal FXR expression (Fig. 5C,D) by 68.7 % and 80.4 %, respectively, relative to the sham group. Oppositely, quinacrine in the (BDL + quinacrine 5) group elevated the expression of liver and hippocampus FXR (1.6-, 2.72-fold), respectively, relative to BDL group. Meanwhile, quinacrine in the (BDL + quinacrine 10) group elevated the expression of liver and hippocampus FXR (2.7-, 3.27-fold), respectively,

relative to BDL group. Moreover, a statistically significant difference was detected between both doses of quinacrine, where co-treatment with quinacrine (BDL + quinacrine 10) elevated expression of liver and hippocampus FXR (1.65-, 1.2-fold), respectively, relative to (BDL + quinacrine 5).

### 3.8. Effect of quinacrine on liver and hippocampal bone morphogenetic protein 2 (BMP2) signaling pathway

#### 3.8.1. Liver

Liver BMP2 (Fig. 5E,F) and P-Smad 1/5/8 (Fig. 5G,H) expression was significantly downregulated in BDL group by 76.4 % and 69.8 %, respectively, opposed to sham group. Nevertheless, hepatic BMP2 and P-Smad 1/5/8 protein levels were substantially raised by 2.16- and 1.61-fold, respectively, in the (BDL + quinacrine 5) treated group. Notably, in

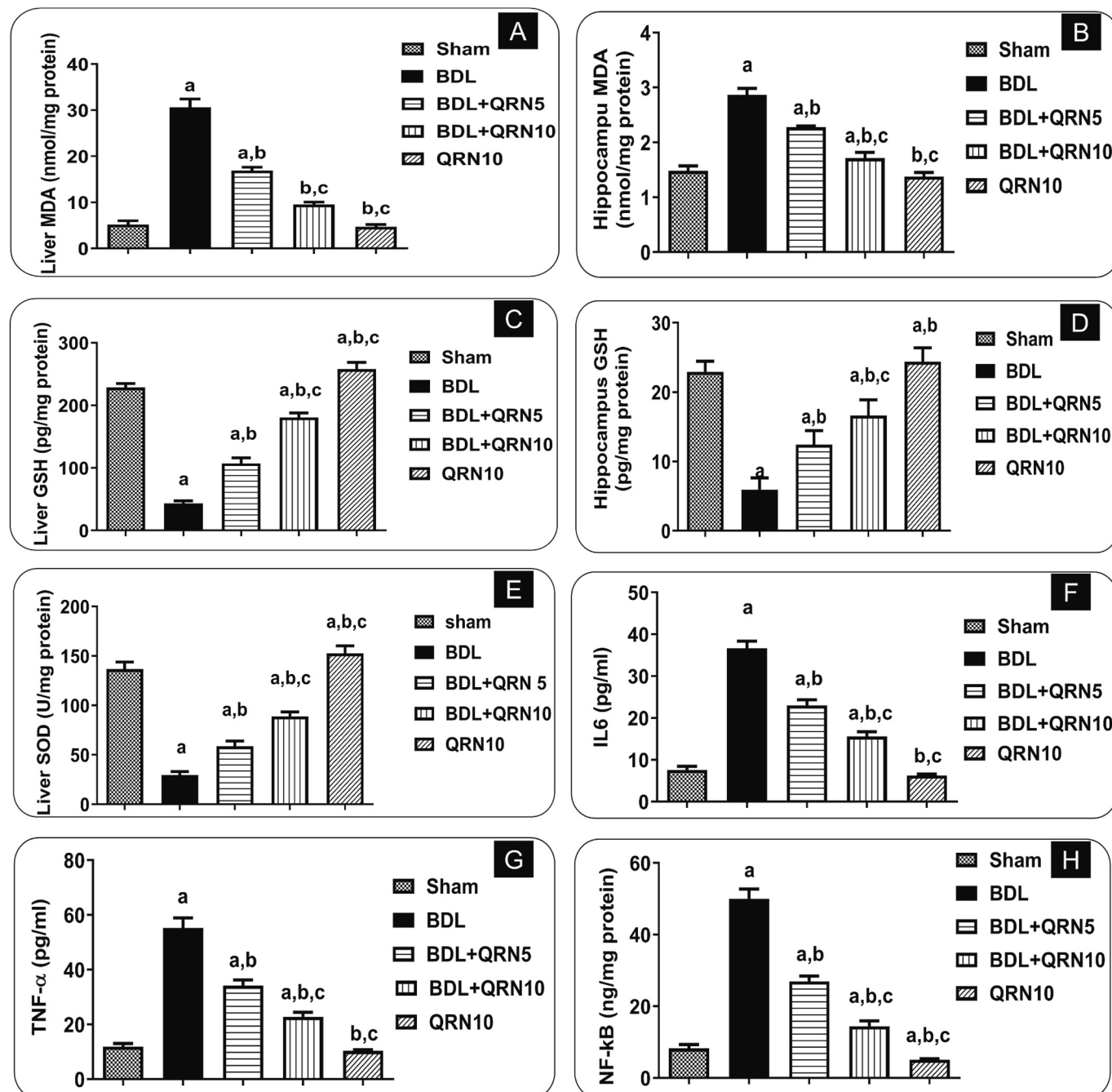


**Fig. 4.** The impact of quinacrine (QRN) on oxidative stress markers, anti-oxidant enzymes, and inflammatory markers in BDL-induced HE. (A) Liver MDA, (B) Hippocampal MDA, (C) Liver MDA, (D) Hippocampal GSH, (E) Liver SOD, (F) Serum IL-6, (G) Serum TNF- $\alpha$  and (H) Liver NF- $\kappa$ B. Data are displayed as mean  $\pm$  SD ( $n = 6$ ). a: vs. sham group, b: vs. BDL group, c: vs. (BDL+QRN5) group at  $p < 0.05$  utilizing one-way ANOVA with Tukey's test as the post-hoc analysis.

the (BDL + quinacrine 10) treated group, there was a notable rise in liver BMP2 and P-Smad 1/5/8 expression (3- and 2.1-fold), respectively, versus the BDL group. Interestingly, there was a substantial distinction between the two doses of quinacrine in BMP2 and P-Smad 1/5/8 expression, where (BDL + quinacrine 10) resulted in a 1.4- and 1.3-fold increase in liver BMP2 and P-Smad 1/5/8 expression, respectively, contrasting to (BDL + quinacrine 5) co-treatment.

### 3.8.2. Hippocampus

The levels of hippocampal BMP2 (Fig. 5I,J) and P-Smad 1/5/8 (Fig. 5K,L) markedly decreased by 76.33 % and 72.7 %, respectively, in BDL group relative to sham group. However, hippocampal BMP2 and P-Smad 1/5/8 expression was substantially raised in the (BDL +

quinacrine 5) treated group, with a 2.27-fold increase for BMP2 and a 1.95-fold increase for P-Smad 1/5/8, comparative to the BDL group. In addition, hippocampal BMP2 and P-Smad 1/5/8 expression was considerably increased in the (BDL + quinacrine 10) treated group, with a 3.38-fold increase for BMP2 and a 2.71-fold increase for P-Smad 1/5/8, relative to BDL group. There was a noteworthy rise in hippocampus BMP2 and P-Smad 1/5/8 expression with fold changes of 1.49 and 1.39, respectively, (BDL + quinacrine 10) treated group versus (BDL + quinacrine 5) treated group.

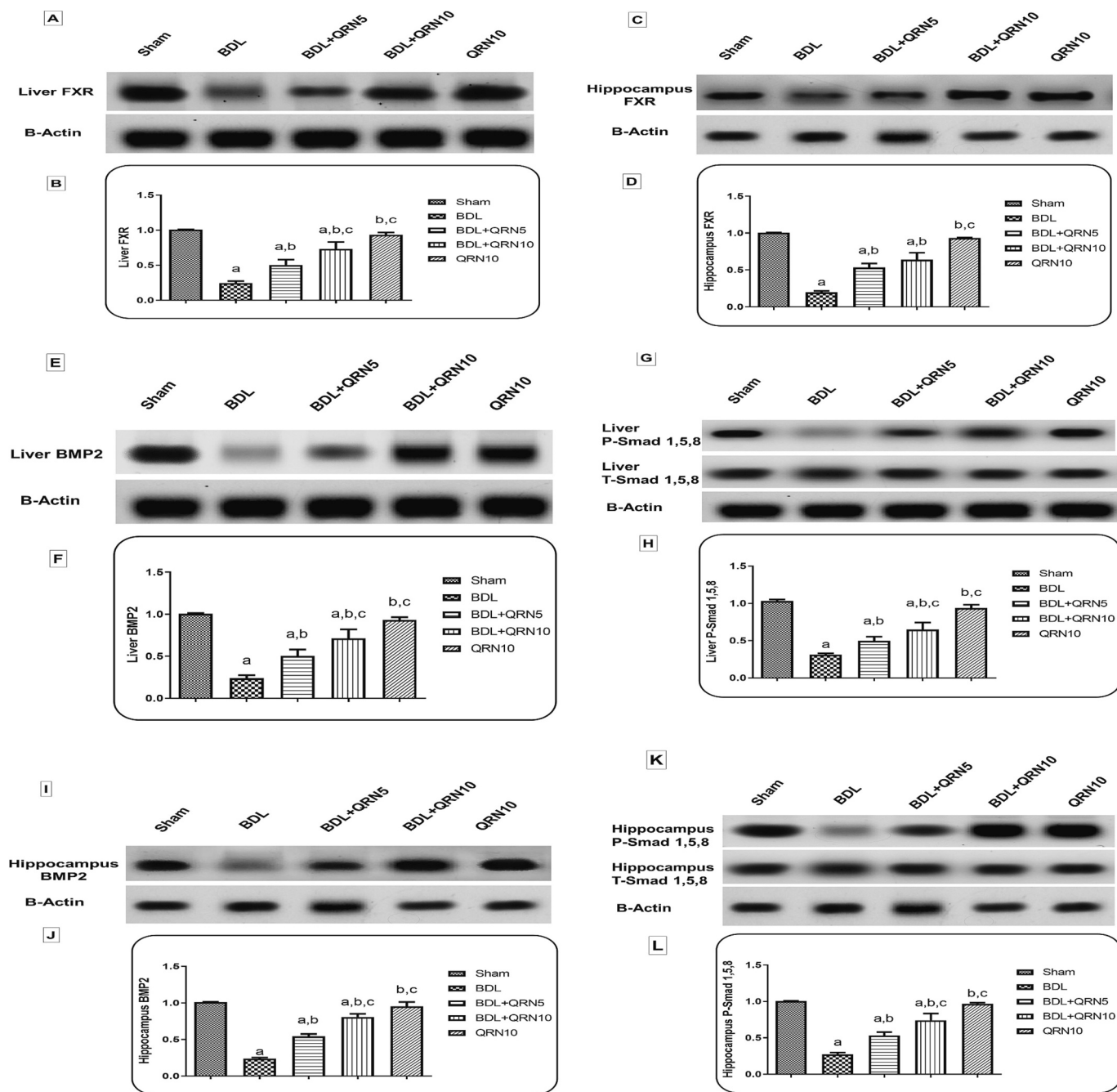


**Fig. 5.** The impact of quinacrine (QRN) on BDL induced alteration in the expression of (A,B) Liver FXR, (C,D) Hippocampal FXR, (E,F) Liver BMP2, (G,H) Liver P-Smad 1/5/8, (I,J) Hippocampal BMP2, (K,L) Hippocampal P-Smad 1/5/8 by western blot analysis. Data are displayed as mean  $\pm$  SD ( $n = 3$ ). a: vs. sham group, b: vs. BDL group, c: vs. (BDL+QRN5) group at  $p < 0.05$  utilizing one-way ANOVA with Tukey's test as the post-hoc analysis.

### 3.9. The impact of quinacrine on hippocampal WNT signaling pathway in BDL rats

In the BDL group, there was a substantial reduction of 77.32 %, 78.9 %, and 71.3 % in the expression of hippocampal WNT3A (Fig. 6A,B),  $\beta$ -catenin (Fig. 6C,D), and Lef1 (Fig. 6E,F), respectively, relative to the sham group. Nevertheless, the (BDL + quinacrine 5) treated group exhibited a significant upregulation in WNT3A,  $\beta$ -catenin, and Lef1 expression with fold changes of 2.5, 2.27, and 1.64, respectively, contrasted to the BDL group. Furthermore, the (BDL + quinacrine 10) treated group exhibited a considerable increase in WNT3A,  $\beta$ -catenin, and Lef1 expression with fold changes of 3.4, 4.49, and 2.86, respectively, opposed to BDL group. In addition, the (BDL + quinacrine 10)

treated group showed a considerable increase in the expression of WNT3A,  $\beta$ -catenin, and Lef1 (1.45-, 1.98-, and 1.74-fold), respectively, in contrast to the (BDL + quinacrine 5) treated group.

### 3.10. Effect of quinacrine on hippocampal brain derived neurotrophic factor (BDNF) expression

Fig. 6G and H demonstrate that BDL led to a considerable decline in BDNF expression by 66.9 % relative to the sham group. Nevertheless, in the (BDL + quinacrine 5) and (BDL + quinacrine 10) treated groups, there was a substantial rise in BDNF expression, with a fold change of 1.49 and 2.62, respectively, relative to the BDL group. Furthermore, there was a noticeable disparity between the two doses of quinacrine.

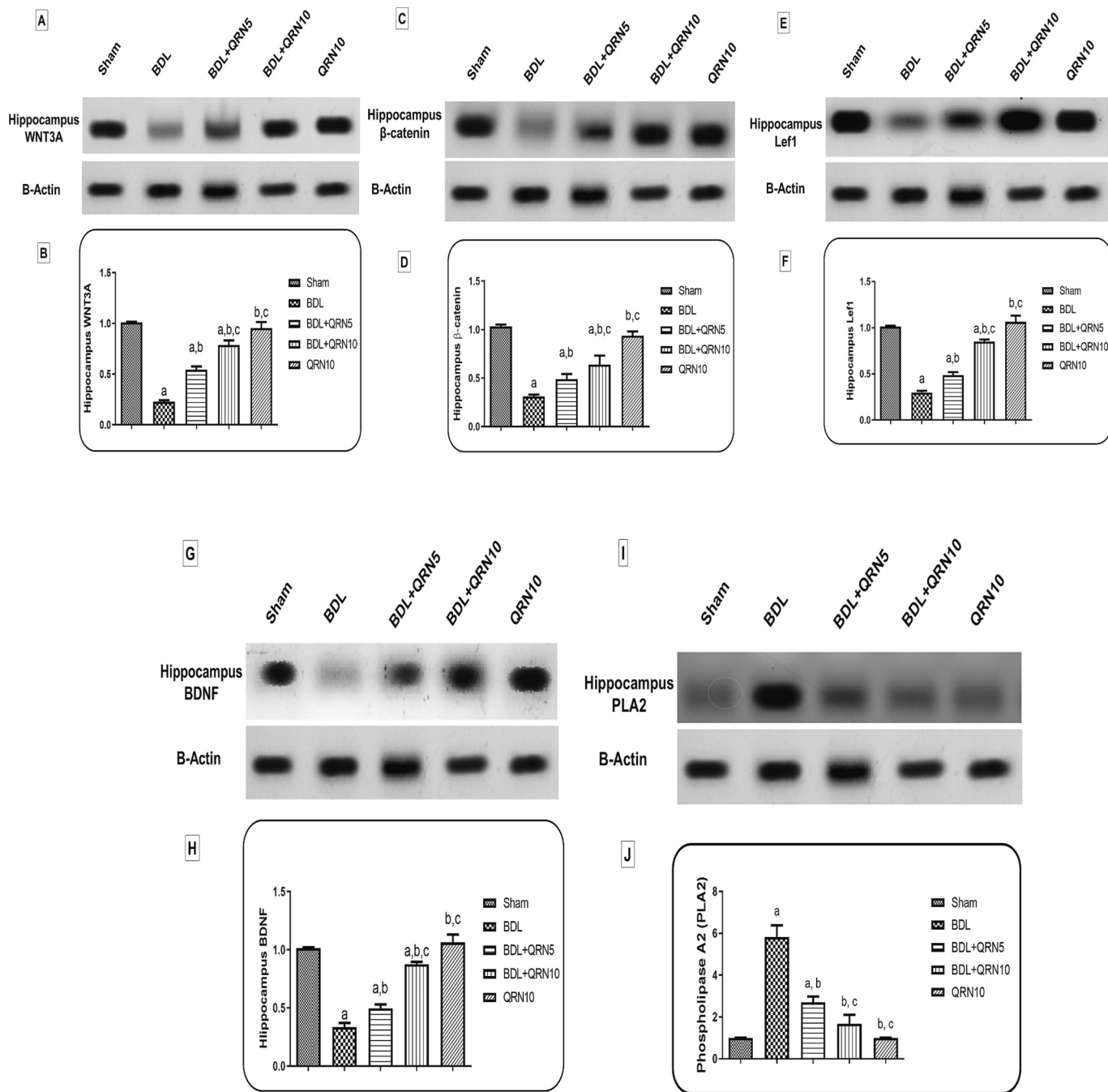


**Fig. 6.** The impact of quinacrine (QRN) on BDL induced alteration in the expression of (A,B) Hippocampal WNT3A, (C,D) Hippocampal  $\beta$ -catenin, (E,F) Hippocampal Lef1, (G,H) Hippocampal BDNF and (I,J) Hippocampal PLA2 by western blot analysis. BDL was conducted on rats, and quinacrine was administered i.p. at doses of 5 and 10 mg/kg daily for a period of 28 days. ( $n = 3$ ), data is displayed as mean  $\pm$  SD. a: vs. sham group, b: vs. BDL group, c: vs. (BDL+QRN5) group at  $p < 0.05$  utilizing one-way ANOVA with Tukey's test as the post-hoc analysis.

(BDL + quinacrine 10) resulted in a 1.76-fold increase in BDNF expression versus co-(BDL + quinacrine 5).

### 3.11. Effect of quinacrine on hippocampal phospholipase A2 (PLA2) expression

In contrast to the sham group, BDL group exhibited a 5.7-fold upregulation in PLA2 expression. Nevertheless, quinacrine administration in the (BDL + quinacrine 5) and (BDL + quinacrine 10) groups, significantly reduced that percentage by 56 % and 73 %, respectively, compared to the BDL group. Furthermore, when compared to the (BDL + quinacrine 5) group, the (BDL + quinacrine 10) group showed a

substantial 39 % drop in PLA2 levels (Fig. 6I,J).

### 3.12. The impact of quinacrine on hepatic fibrosis markers

The BDL group had a 22.8-fold higher level of TGF- $\beta$ 1 in comparison to the sham group. Nevertheless, opposed to the BDL group, quinacrine substantially lowered TGF- $\beta$ 1 tissue levels in the (BDL + quinacrine 5) and (BDL + quinacrine 10) groups by 33.74 % and 86.9 %, respectively. It should be noted that the one that (BDL + quinacrine 10) group exhibited an 80.2 % drop in TGF- $\beta$ 1 opposed to (BDL + quinacrine 5) group (Fig. 7). Likewise, BDL group exhibited an 8.7-fold increase in  $\alpha$ -SMA when contrasted with the sham group. Alternatively, in

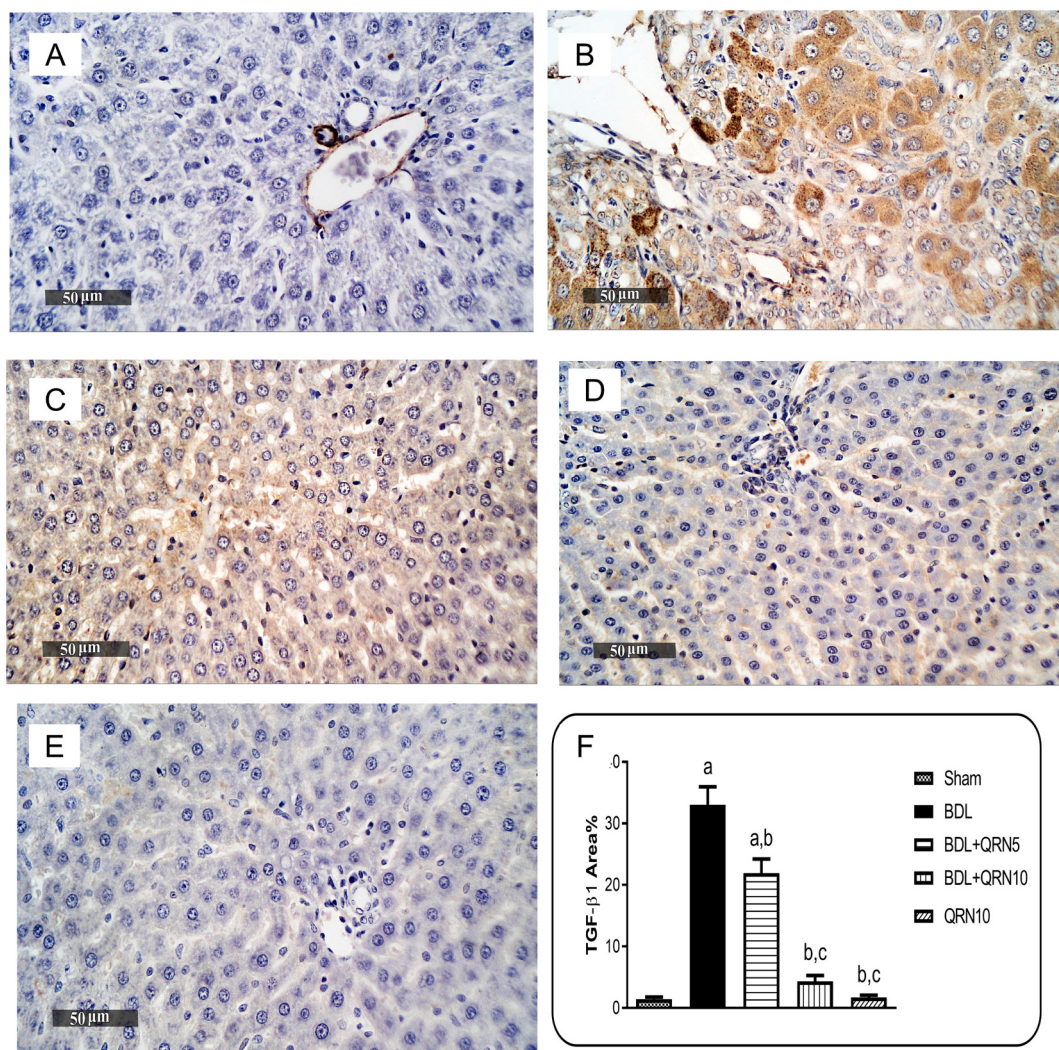


**Fig. 7.** The impact of quinacrine (QRN) on the expression of TGF- $\beta$ 1 in rats with BDL-induced HE was assessed by evaluating the immunostaining reaction, indicated by the presence of brown colour in hepatic tissue. (A) sham group, (B) BDL group, (C) BDL+QRN5 group, (D) BDL+QRN10 group and (E) QRN10 group. (F) Quantitative image analysis is measured by calculating the proportion of the area that shows immunopositive reaction. Data are displayed as mean  $\pm$  SD ( $n = 3$ ). a: vs. sham group, b: vs. BDL group, c: vs. (BDL+QRN5) group at  $p < 0.05$  utilizing one-way ANOVA with Tukey's test as the post-hoc analysis.

comparison to the BDL group, quinacrine therapy considerably decreased  $\alpha$ -SMA by 79.2 % and 82.5 % in the (BDL + quinacrine 5) and (BDL + quinacrine 10) groups, respectively. Interestingly, neither of the quinacrine doses showed a notable variation in  $\alpha$ -SMA levels (Fig. 8). In addition, the hydroxyproline content assessment of collagen showed that the BDL group had a 9.88-fold higher hydroxyproline level than the sham group. The (BDL + quinacrine 5) and (BDL + quinacrine 10) groups showed a greatly lowered hydroxyproline content relative to the BDL group, by 45 % and 77.35 %, respectively. While (BDL + quinacrine 10) group had a considerably lower hydroxyproline content (58.82 %) than (BDL + quinacrine 5) group (Fig. 9). Furthermore, Masson's trichrome staining was used to show that distinct experimental groups' hepatic tissues had collagen deposition (Fig. 9). (Fig. 9A, E) reveal that the sham group and the (quinacrine 10 + sham) group had minimal collagen deposition. As seen in Fig. 9B, the BDL group, on the other hand, displayed substantial buildup of collagen fibers in the transitional spaces between the recently formed bile ductules (Fig. 9B), the (BDL + quinacrine 5) group had moderate collagen deposition (Fig. 9C). (BDL + quinacrine 10) group showed reduced collagen deposition (Fig. 9D).

### 3.13. Effect of quinacrine on hippocampal glial fibrillary acidic protein (GFAP) expression in BDL rats

In contrast to the sham group, the BDL group had a GFAP level that was 4-fold higher. In contrast to the BDL group, quinacrine significantly reduced GFAP levels in the (BDL + quinacrine 5) and (BDL + quinacrine 10) groups by 33.9 % and 55.56 %, respectively. In addition, the GFAP level was 33.33 % lower in the (BDL + quinacrine 10) group as compared to the (BDL + quinacrine 5) group (Fig. 10).

### 3.14. Histopathological assessment

#### 3.14.1. Liver

There were no abnormalities in the histology of the rat liver parenchyma in the sham samples, which showed numerous healthy hepatocytes and few signs of degeneration. The hepatic veins and sinusoids were also clearly visible (Fig. 11 A,B). On the other hand, BDL samples showed marked disruption of hepatocellular architecture with significant periportal and interlobular fibroblastic activity with higher collagen deposition accompanied with marked mononuclear inflammatory cells infiltrates. Marked cholangial proliferation was shown with severely dilated hepatic blood vessels (Fig. 11 C,D). The (BDL+

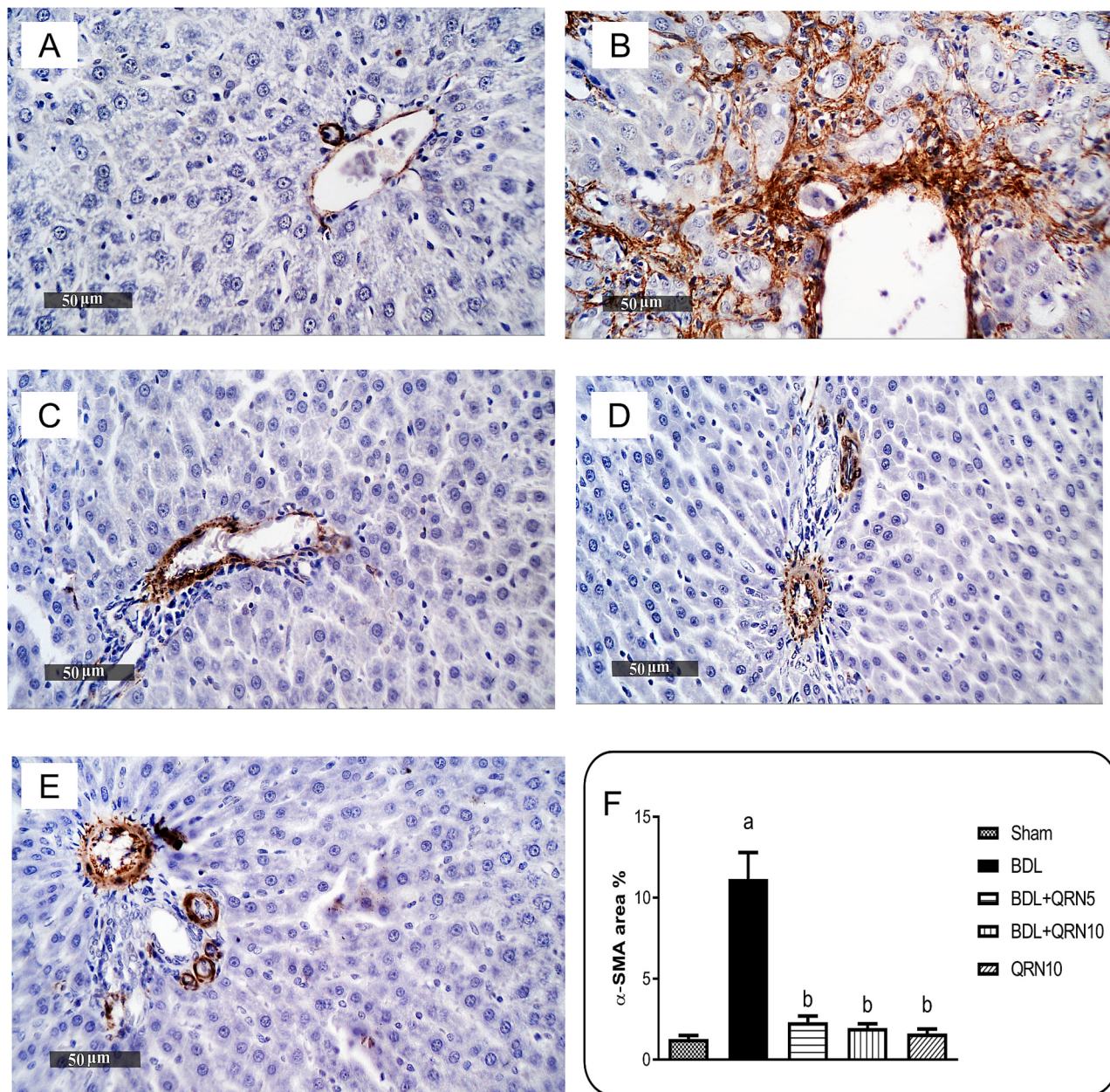


**Fig. 8.** The impact of quinacrine (QRN) on the expression of  $\alpha$ -SMA in rats with BDL-induced HE was assessed by evaluating the immunostaining reaction, indicated the presence of brown colour in the hepatic tissue. (A) sham group, (B) BDL group, (C) BDL+QRN5 group, (D) BDL+QRN10 group and (E) QRN10 group. (F) Quantitative image analysis is measured as the proportion of the immunopositive reaction region. Data are displayed as mean  $\pm$  SD ( $n = 3$ ). a: vs. sham group, b: vs. BDL group, c: vs. (BDL+QRN5) group at  $p < 0.05$  utilizing one-way ANOVA with Tukey's test as the post-hoc analysis.

quinacrine 5) samples showed significant diminished fibroblastic activity with moderate periportal fibrous tissue records with moderate periportal inflammatory infiltrates, and mild persistent bile ductular proliferation were observed in some samples. This together with moderate congested/dilated hepatic blood vessels (Fig. 11 E,F). However, the (BDL+ quinacrine 10) samples showed more apparent hepatoprotective efficacy than low dose samples with apparent intact hepatic parenchyma resembling sham samples (Fig. 11 G,H). The (quinacrine 10 + sham) samples demonstrated almost intact histological features of hepatic parenchyma resembling normal controls without abnormal morphological changes (Fig. 11 I,J).

#### 3.14.2. Hippocampus

The sham samples exhibited typical and well-structured microscopic characteristics of the hippocampal layers, including intact pyramidal

neurons with preserved nuclear and cytoplasmic properties. Additionally, the intercellular brain matrix appeared normal without any aberrant cellular infiltrations (Fig. 12A). On the contrary, the BDL samples exhibited significant neuronal loss and injury, as seen by several instances of degenerated pyknotic pyramidal neurons that had lost their subcellular features. Additionally, there were minor infiltrations of reactive glial cells and modest vacuolization of the brain matrix (Fig. 12B). The (BDL+ quinacrine 5) samples exhibited consistent evidence of neuronal injury interspersed with somewhat higher numbers of undamaged cells and modest infiltration of reactive glial cells. (Fig. 12C). The neuroprotective efficacy of the (BDL+ quinacrine 10) samples was clearly higher, and there were only rare cases of aberrant degenerative alterations in the samples. The intercellular brain matrix was also intact, and there were very few reactive glial cell infiltrates (Fig. 12D). Samples treated with (quinacrine 10 + sham) showed nearly

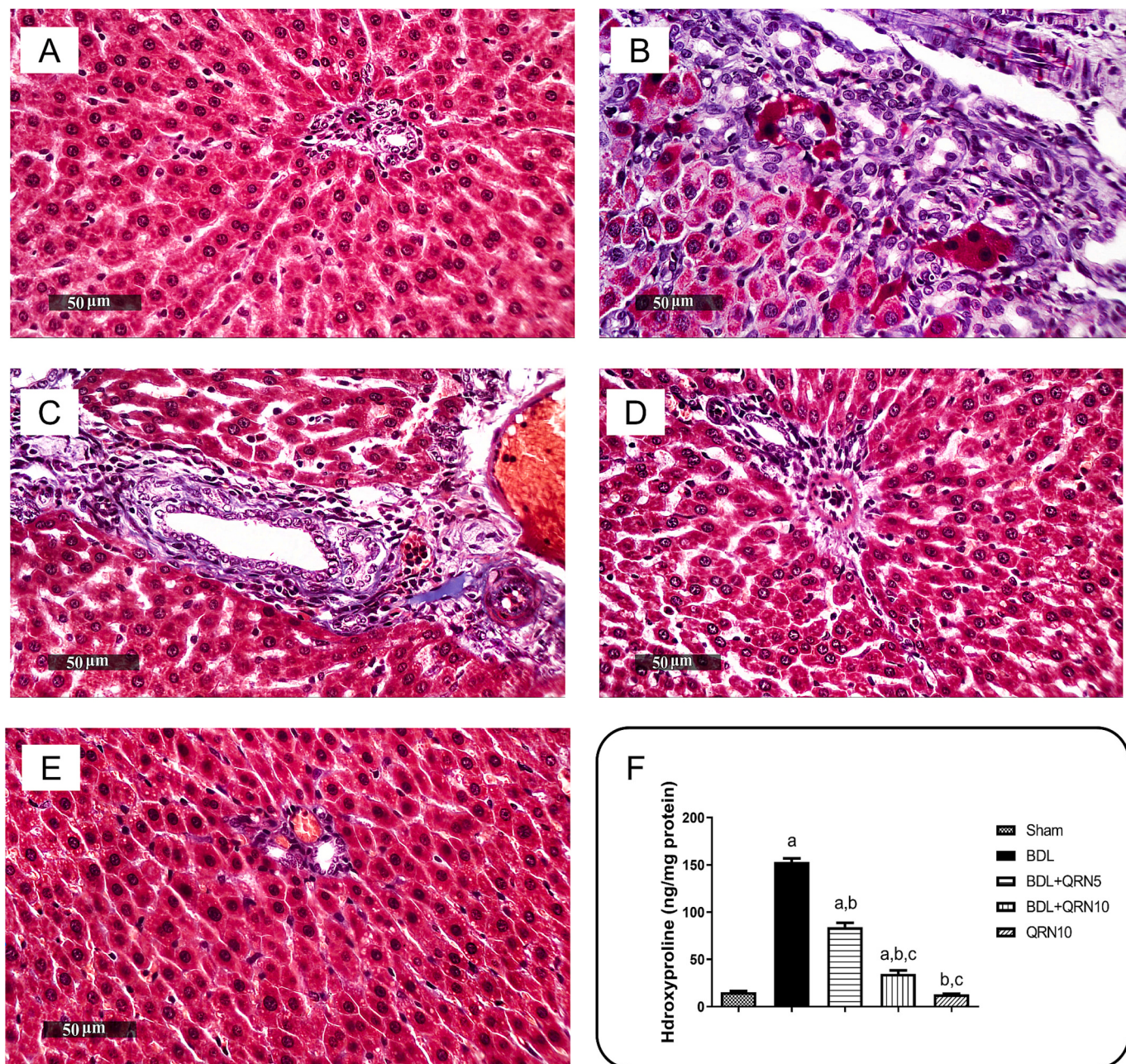


**Fig. 9.** The impact of quinacrine (QRN) on collagen accumulation in the liver tissues with collagen was assessed using Masson's trichrome staining and hydroxyproline quantification. (A:E) Photomicrographs represent Masson's trichrome staining. (A) sham group, (B) BDL group, (C) BDL+QRN5 group, (D) BDL+QRN10 group and (E) QRN10 group. (F) Hepatic hydroxyproline levels in various groups. Data are displayed as mean  $\pm$  SD ( $n = 3$ ). a: vs. sham group, b: vs. BDL group, c: vs. (BDL+QRN5) group at  $p < 0.05$  utilizing one-way ANOVA with Tukey's test as the post-hoc analysis.

identical results to sham samples, meaning no aberrant histological alterations were detected (Fig. 12E).

#### 4. Discussion

Hepatic encephalopathy (HE) is a distinct form of brain dysfunction commonly associated with liver cirrhosis. It is marked by a wide array of generalized neurological and mental health problems [30]. One of the primary contributors to HE is cholestasis, which disrupts bile flow and leads to the accumulation of harmful bile acids in the liver. This condition also impairs the liver's ability to detoxify ammonia, resulting in elevated ammonia levels in both the liver and bloodstream. The accumulation of bile acids and ammonia damages liver cells, initiating oxidative stress and inflammatory reactions, ultimately leading to

hepatic fibrosis. These interconnected processes contribute to the development of neuroinflammation, astrocyte swelling and HE through various pathways [5,31]. In addition, oxidative stress and inflammation can disrupt BMP2 and WNT3A pathways resulting in exaggerated cognitive impairments in HE [11,32,33]. To investigate the impact of quinacrine on these different pathways in HE, this study utilized the BDL model.

The BDL model resulted in significant elevations in liver enzyme activities, hyperammonemia, and hyperbilirubinemia after 28 days, in accordance with previous research [19], where the same model was employed to induce cholestatic liver injury and dysfunction. Quinacrine administration, particularly at the higher dose (10 mg/kg), notably reduced serum levels of various liver markers, suggesting the role of quinacrine in alleviating hepatic injury and cholestasis. The effect of

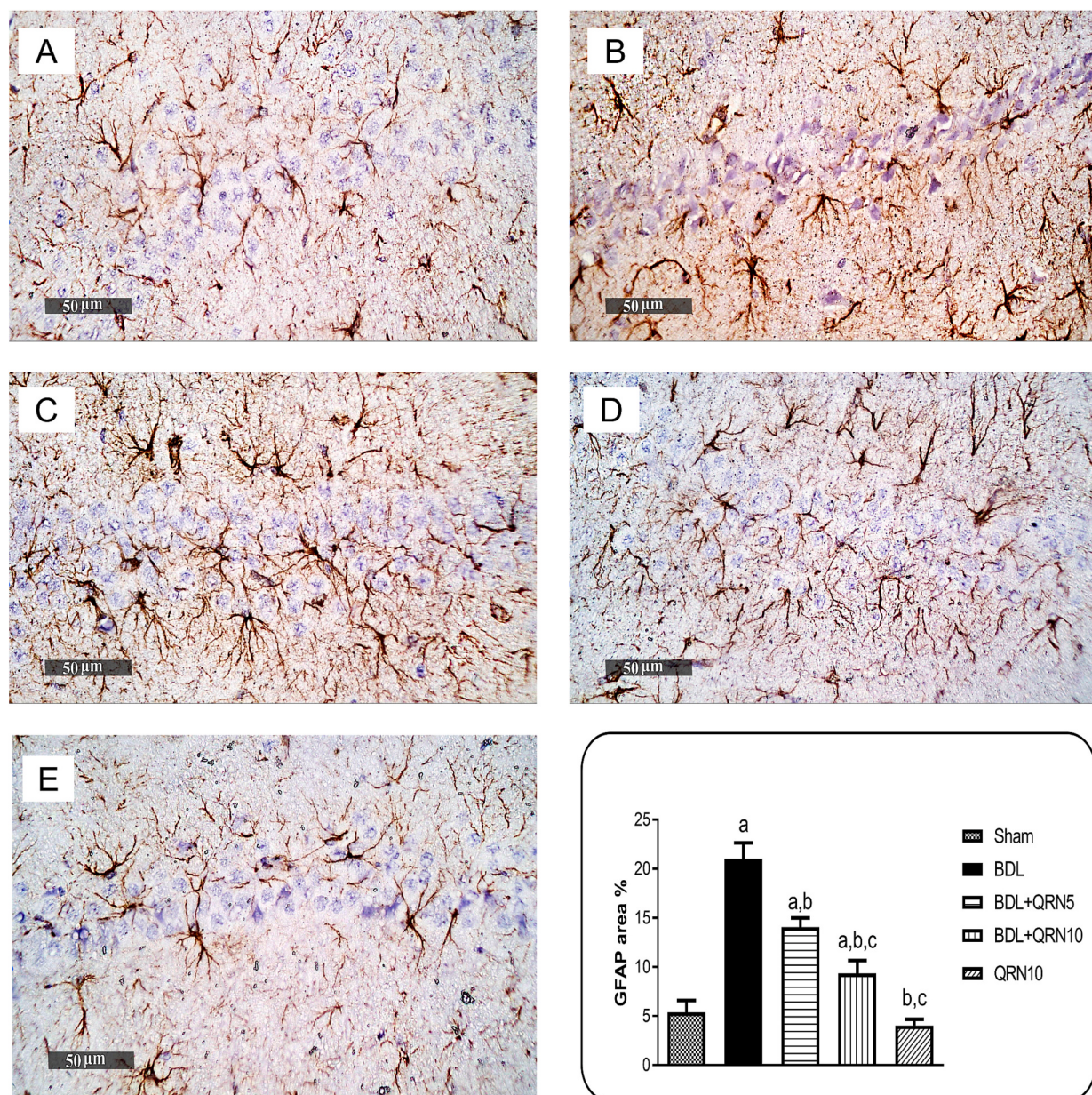


**Fig. 10.** The impact of quinacrine (QRN) on the expression of GFAP in rats with BDL-induced HE was assessed by evaluating the immunostaining reaction, indicated the presence of brown colour in the hippocampus tissue. (A) sham group, (B) BDL group, (C) BDL+QRN5 group, (D) BDL+QRN10 group and (E) QRN10 group. (F) Quantitative image analysis is measured as the proportion of the area showing a positive reaction to immunostaining. Data are displayed as mean  $\pm$  SD ( $n = 3$ ). a: vs. sham group, b: vs. BDL group, c: vs. (BDL+QRN5) group at  $p < 0.05$  utilizing one-way ANOVA with Tukey's test as the post-hoc analysis.

quinacrine on AST and ALT was consistent with previous research [34].

Besides, BDL can result in the buildup of bile acids, that can induce oxidative stress and inflammation, resulting in cholestatic liver fibrosis. Additionally, bile acids can disrupt BBB permeability resulting in neuroinflammation [35]. The FXR has a crucial function in regulating the balance of bile acids by inhibiting their production and buildup. Disruption of bile acid levels in the brain initially leads to FXR upregulation, followed by downregulation, contributing to bile acid buildup. This buildup directly impacts neurological deterioration, highlighting the relationship between FXR, bile acids, and neurological health [36]. Additionally, FXR has been shown to impact inflammatory process through decreasing the proinflammatory cytokines including TNF- $\alpha$  and IL-6. Moreover, FXR activation can reduce oxidative stress by enhancing the expression of antioxidant genes [37]. The present study showed that FXR expression was notably suppressed in liver and hippocampal tissues in the BDL group in alignment with earlier research [38]. Tissue FXR

was significantly increased when quinacrine doses were administered, proposing quinacrine reducing the effects of neurological decline.

Oxidative stress triggered from bile acids accumulation results in hepatocellular damage. The elevated oxidative stress resulting from BDL-induced liver injury can also disrupt the antioxidant homeostasis of the brain through systemic circulation in adult animals [39]. The present study demonstrated a noticeable decrease in antioxidant levels in rats that received the BDL operation, which comes in alignment with previous studies [31,40]. Quinacrine counteracted these effects, in conformity with a prior investigation in experimental models of acute kidney injury [14] and status epilepticus [13].

Essentially, the build-up of harmful bile acids and resulting rise in oxidative stress after BDL can cause an inflammatory reaction and stimulate the production of inflammatory mediators (IL-6, TNF- $\alpha$  and NF- $\kappa$ B) in the liver [41]. This process serves as vital for the progression of liver damage, fibrosis and HE. Substantial elevations of inflammatory

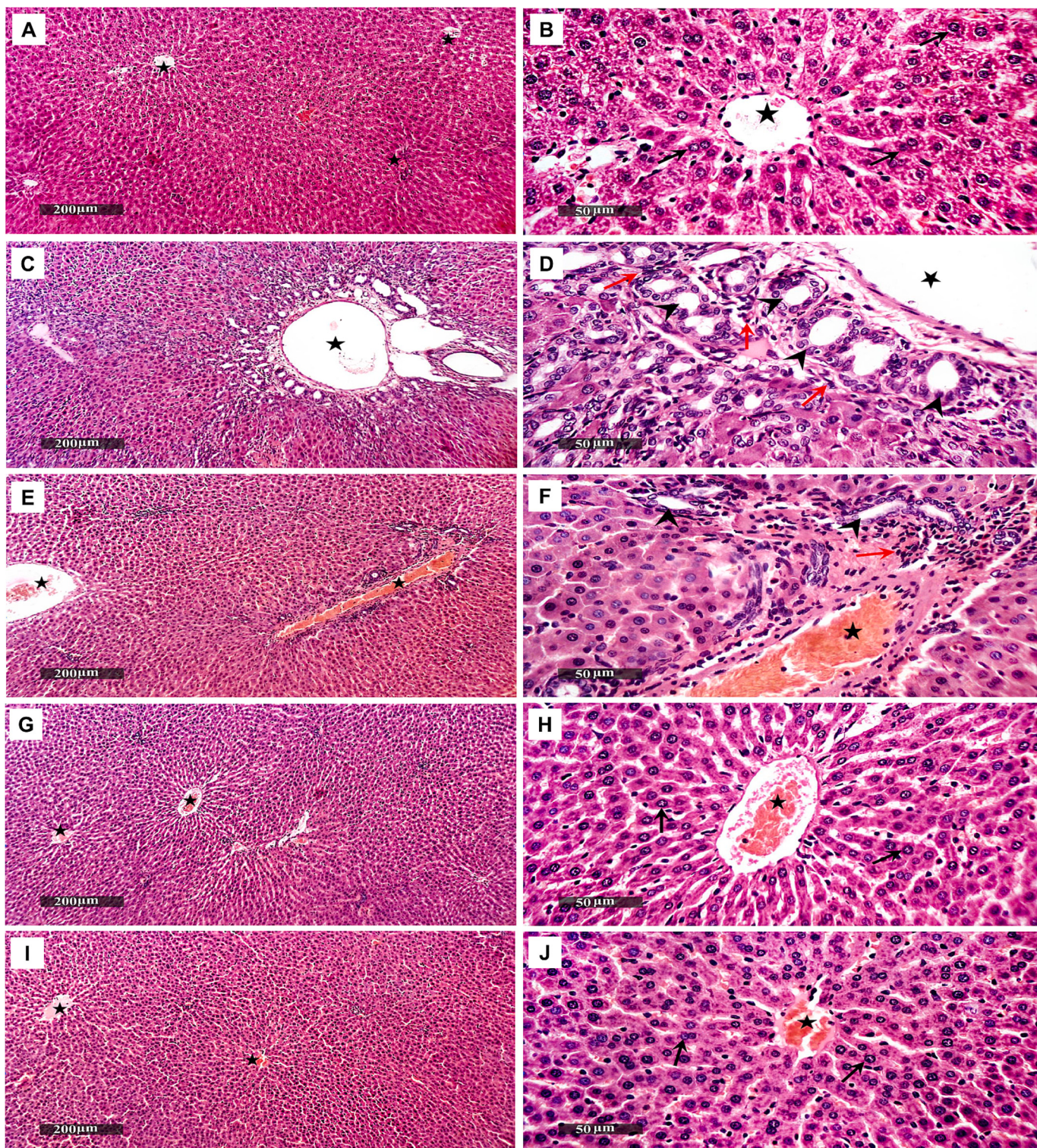


**Fig. 11.** The impact of quinacrine (QRN) on BDL induced hepatic histological alterations in HE (hematoxylin and eosin staining) ( $n = 3$ ). (A,B) sham group, (C,D) BDL group, (E,F) BDL+QRN5 group, (G,H) BDL+QRN10 group and (I,J) QRN10 group. Apparent intact well-organized hepatocytes with intact subcellular details (shown by black arrow), inflammatory cells infiltrate (shown by red arrow), hepatic blood vessels. (star) and cholangiolar proliferation (shown by arrow head).

mediators in BDL animals were reported in the current study in conjunction with a previous study [6]. It was observed that quinacrine led to a substantial reduction in their levels. Prior studies have documented the inhibitory impact of quinacrine on TNF- $\alpha$ , IL-6, and NF- $\kappa$ B. [12,42]. These results illustrate quinacrine anti-inflammatory and antioxidant actions.

Astrocytes are specialized glial cells in the CNS that contribute to the

structural integrity of the brain, uphold the BBB and protect against neurotoxins like ammonia [43]. Elevated ammonia levels can lead to excessive glutamine accumulation within astrocytes, causing ionic imbalances and swelling, which significantly contributes to brain edema associated with HE [44] [45]. Additionally, in response to brain tissue damage, astrocytes undergo astrogliosis, characterized by increased production GFAP [46]. GFAP is a frequent histological finding in the

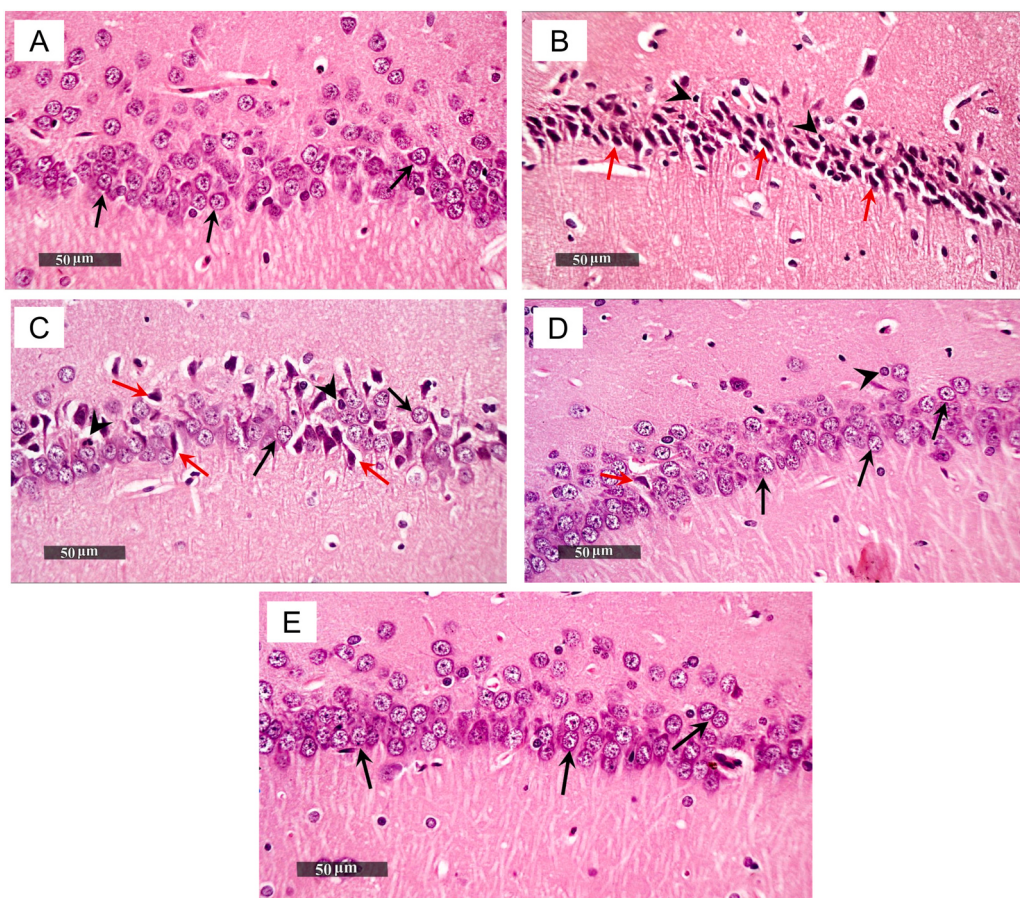


**Fig. 12.** The impact of quinacrine (QRN) on BDL induced hippocampal histological alterations in HE (hematoxylin and eosin staining) ( $n = 3$ ). (A) sham group, (B) BDL group, (C) BDL+QRN5 group, (D) BDL+QRN10 group and (E) QRN10 group. Neurons with intact nuclear and cytoplasmic details (shown by the black arrow), degenerated pyknotic pyramidal neurons losing their subcellular details (shown by the red arrow) and reactive glial cell infiltration (indicated by the arrow head).

brains of individuals affected by HE [47]. This is in line with the present study results which observed a significantly elevated GFAP expression in the hippocampus of BDL rats. Quinacrine administration resulted in a substantial reduction in its expression. Additional research is recommended to clarify the precise mechanism by which quinacrine reduces GFAP expression.

When cerebral endothelial cells in the BBB are exposed to toxins, such as ammonia, they can potentially activate a variety of inflammatory factors, including PLA2, which is a precursor for various inflammatory mediators, including prostaglandins and leukotrienes, which can exacerbate inflammation and contribute to the swelling of astrocytes in HE. [48]. This lines up with the findings of the present study where PLA2 expression was markedly elevated in the BDL group. Interestingly, administration of quinacrine significantly reduced PLA2 expression. This conforms with other studies which reported the inhibitory effect of quinacrine on PLA2 in several experimental models [14,49].

Hepatic fibrosis serves as a critical progression step from liver injury to HE. TGF- $\beta$ 1 and BMP2 are two essential cytokines that exert opposing effects in the regulation of fibrosis, highlighting their complex relation in hepatic fibrosis [8]. TGF- $\beta$ 1 is essential in progression of hepatic fibrosis. It stimulates hepatic stellate cells (HSCs) to express  $\alpha$ -SMA, a marker of myofibroblast differentiation which can produce and deposit extracellular matrix (ECM) proteins, containing collagen, which has the potential to the formation and advancement of hepatic fibrosis [50]. TGF- $\beta$ 1 signal through binding to its receptors, leading to the phosphorylation of SMAD2 and SMAD3, which then form a complex with SMAD4. This complex translocates to the nucleus to regulate the transcription of genes associated with fibrosis. While BMP2, upon binding to its receptors BMPRIs and BMPRIIs, it activates the phosphorylation

factors Smad 1/5/8, enabling their association with the common mediator Smad4, resulting in the transactivation of target genes [7]. BMP2 has been demonstrated to counteract the fibrotic effects induced by TGF- $\beta$ 1 via inhibiting the phosphorylation of SMAD2 and SMAD3. Additionally, BMP2 can also inhibit the expression of SMAD7, which is an inhibitory SMAD that negatively regulates TGF- $\beta$ 1 signaling. This interplay highlights the regulatory role of BMP2 in modulating fibrosis [51,52]. The present study found that rats subjected to BDL showed a notable increase in hepatic fibrotic markers consistent with findings from a recent study that also used the BDL model [53]. These effects were considerably mitigated by quinacrine treatment. Furthermore, BDL rats showed a notable decline in BMP2 and P-Smad 1/5/8 expression aligned with previous reports [8,54]. Interestingly, quinacrine restored BMP2 and P-Smad 1/5/8 expression which was responsible for attenuating TGF- $\beta$ 1 activation and thus restraining fibrosis. The effect of quinacrine on BMP2 and P-Smad 1/5/8 was reported in a previous study [15].

Additionally, BMP2 can also exert a neuroprotective effect [15]. Oxidative stress and inflammation can disrupt brain BMP2-P-Smad 1/5/8 and WNT3A pathways [11,32,33], which are crucial in neuronal health and survival [9] resulting in the cognitive impairments associated with HE. Conversely, activating the WNT3A pathway may reduce BBB damage, lower neuroinflammation, and alleviate the effects triggered by oxidative stress (Xingyong [32]). Moreover, restoring BMP2 can alleviate inflammation [55]. The current study demonstrated that rats that underwent BDL showed a notable decrease in hippocampal BMP2, P-Smad 1/5/8, WNT3A, Lef1, and  $\beta$ -catenin expression. It is worth noting that quinacrine, when administered led to a notable recovery of their expression. The neuroprotective potential of quinacrine via modulation

BMP2 and P-Smad 1/5/8 was previously shown [15].

BDNF is widely acknowledged to play a central role in long-term potentiation, learning, and memory processes in the hippocampus. It regulates both the immediate, short-term changes in synaptic function and the long-lasting, activity-dependent changes in synaptic plasticity in the adult hippocampus [56,57]. Ammonia and neuroinflammation downregulates the expression of BDNF in the hippocampus contributing to memory and learning impairment in HE patients [58]. Moreover, various studies suggested that BMPs may exhibit cooperative interaction with other neurotrophic factors to exert neurotrophic effects. For instance, BMP-2 has been shown to function synergistically with BDNF or neurotrophin-3 (NT-3) [59]. The current study demonstrated that BDL was notably associated with low expression of BDNF, in line with an earlier study [6]. Noteworthy, its expression was considerably raised with quinacrine, emphasizing the neuroprotective effect of quinacrine.

Finally, rats that underwent BDL showed cognitive deficits. The present investigation involved the conduction of the MWM and NOR tests. The cognitive impairments observed in BDL rats are evidenced by deficits in spatial learning and memory in the MWM and impaired recognition NOR test. These findings align with previous research that has similarly documented cognitive impairments in BDL rats [22,60] [61]. Quinacrine mitigated the cognitive impairments caused by BDL, indicating the potential of quinacrine in preventing the decline in learning and memory capabilities in BDL rats. Evaluation of locomotor activity and anxiety levels using the OF test showed no significant changes post-BDL, which aligns with a prior investigation [62].

The findings of histological investigation have provided support for the outcomes of the current study. Histological examinations of the liver in the BDL group showed several abnormalities which were consistent with earlier research [63]. Quinacrine administration reduced fibroblastic activity, fibrous tissue deposition, and inflammatory infiltrates, where the 10 mg/kg dose samples showed more hepatoprotective effectiveness, preserving hepatic parenchyma. This introduced the potential of quinacrine in mitigating hepatic histopathological changes. Moreover, the histological analysis of the hippocampus tissues unveiled a substantial neuron loss and degeneration, in conjunction with a recent study [19]. While quinacrine administration preserved more intact cells and reduced neuronal injury.

## 5. Conclusion

Quinacrine exhibited protective effects in both the liver and hippocampus in HE induced by BDL. Quinacrine administration, particularly the higher dose (10 mg/kg) effectively reduced bilirubin, ammonia, liver enzyme levels, oxidative stress markers, and inflammatory mediators, hepatic fibrosis markers, and hippocampal GFAP, thereby inhibiting fibrosis progression and astrocyte activation. Additionally, quinacrine enhanced signaling pathways related to liver and hippocampal health, including BMP2, FXR in both organs and WNT3A Pathway in the hippocampus. Also, it enhanced hippocampal BDNF, showcasing its comprehensive protective actions in both organs.

## CRediT authorship contribution statement

**Manar M. Esmail:** Writing – review & editing, Writing – original draft, Methodology, Investigation, Data curation, Conceptualization. **Noha M. Saeed:** Writing – review & editing, Supervision, Methodology, Conceptualization. **Diana M.F. Hanna:** Writing – review & editing, Supervision, Methodology, Conceptualization. **Haidy E. Michel:** Writing – review & editing, Supervision, Methodology, Conceptualization. **Reem N. El-Naga:** Writing – review & editing, Supervision, Methodology, Conceptualization. **Samar S. Azab:** Writing – review & editing, Supervision, Methodology, Conceptualization.

## Author contributions

Manar M. Esmail: Conception and design, acquisition of data, analysis and interpretation of the results, writing the initial draft of the article, and reviewing and approving the final version of the paper.

Noha M. Saeed: Conception and design, analysis and interpretation of the results, reviewing and approving the final version of the paper.

Diana M.F. Hanna: Conception and design, analysis and interpretation of the results, reviewing and approving the final version of the paper.

Haidy E. Michel: Conception and design, analysis and interpretation of the results, reviewing and approving the final version of the paper.

Reem N. El-naga: Conception and design, analysis and interpretation of the results, reviewing and approving the final version of the paper

Samar S. Azab: Conception and design, analysis and interpretation of the results, reviewing and approving the final version of the paper.

## Authorship statement

The authorship statement of the journal has been read by all of the authors, and they all agree with it.

## Consent to participate

Not applicable.

## Consent for publication

All authors have perused and have agreed to the authorship statement of the journal. In accordance with the rules of your publication, we hereby verify that the material of the paper is authentic and has not been previously published or submitted elsewhere. The authors are duly qualified and do not have any financial or personal conflicts of interest. The guidelines for online submission are applicable to this paper.

The Authors confer upon the Journal both exclusive rights to the manuscript, any revisions made, and copyright protection. The Journal possesses the following rights: (1) authorization to duplicate, publish, sell, and distribute copies of the manuscript, selected portions of the manuscript, as well as translations and other derivative works derived from the manuscript in print, audio-visual, electronic, or any other media currently or in the future; (2) authorization to reprint the manuscript to third parties for educational photocopying; (3) authorization to others to generate abstracts and indexes; and (4) authorization to secondary publishers. Exclusive rights shall be applicable during the copyright period, as well as during any renewals and extensions.

## Ethics approval

All animal experimental procedures were approved by the Ain Shams University Research Ethics Committee (ACUC-FP-ASU RHDIB-B2020110301REC#106) in Egypt and conducted in compliance with their regulations.

## Funding

This research did not get any dedicated support from public, commercial, or not-for-profit organizations.

## Declaration of competing interest

The authors have carefully read the journal's policy regarding the disclosure of potential conflicts of interest. They collectively affirm that there are no known conflicts of interest related to this publication, and there has been no substantial financial backing for this research that could have influenced its results.

## Acknowledgments

The authors express their gratitude for the technical assistance provided by Dr. Mohamed Abdelrazik Khattab, a Professor in Cytology and Histology and at the Faculty of Veterinary Medicine, Cairo University, in conducting the histopathological analysis and immunostaining of the samples. Additionally, Dr. Laila A Rashed from the Department of Medical Biochemistry, Molecular Biology, and Tissue Engineering Unit at the Faculty of Medicine, Cairo University in Cairo, Egypt, for her assistance with the technical aspects of ELISA and western blotting.

## Code availability

Not applicable.

## Appendix A. Supplementary data

Supplementary data to this article can be found online at <https://doi.org/10.1016/j.lfs.2024.123229>.

## Data availability

Data will be made available on request.

## References

- [1] C.F. Rose, P. Amadio, J.S. Bajaj, R.K. Dhiman, S. Montagnese, S.D. Taylor-Robinson, H. Vilstrup, R. Jalan, Hepatic encephalopathy: novel insights into classification, pathophysiology and therapy, *J. Hepatol.* 73 (6) (2020) 1526–1547, <https://doi.org/10.1016/j.jhep.2020.07.013>.
- [2] S. Baghbaderani, M. Hashemi, M. Ebrahimi-Ghiri, M.R. Zarrindast, M. Nasehi, M. Entezari, Curcumin prevents cognitive deficits in the bile duct ligated rats, *Psychopharmacology* 237 (12) (2020) 3529–3537, <https://doi.org/10.1007/s00213-020-05633-6>.
- [3] R. Ochoa-Sánchez, F. Tamnanloo, C.F. Rose, Hepatic encephalopathy: from metabolic to neurodegenerative, *Neurochem. Res.* 46 (10) (2021) 2612–2625, <https://doi.org/10.1007/s11064-021-03372-4>.
- [4] I. Coltart, T.H. Tranah, D.L. Shawcross, Inflammation and hepatic encephalopathy, *Arch. Biochem. Biophys.* 536 (2) (2013) 189–196, <https://doi.org/10.1016/j.abb.2013.03.016>.
- [5] C. D'Mello, M.G. Swain, Liver-brain inflammation axis, *Am. J. Physiol. Gastrointest. Liver Physiol.* 301 (5) (2011) G749–G761, <https://doi.org/10.1152/ajpgi.00184.2011>.
- [6] S. Dhandha, S. Gupta, A. Halder, A. Sunkaria, R. Sandhir, Systemic inflammation without gliosis mediates cognitive deficits through impaired BDNF expression in bile duct ligation model of hepatic encephalopathy, *Brain Behav. Immun.* 70 (2018) 214–232, <https://doi.org/10.1016/j.bbi.2018.03.002>.
- [7] T.K. Sampath, A.H. Reddi, Discovery of bone morphogenetic proteins - A historical perspective, *Bone* 140 (2020) 115548, <https://doi.org/10.1016/j.bone.2020.115548>.
- [8] Y.H. Chung, Y.H. Huang, T.H. Chu, C.L. Chen, P.R. Lin, S.C. Huang, D.C. Wu, C. C. Huang, T.H. Hu, Y.H. Kao, M.H. Tai, BMP-2 restoration aids in recovery from liver fibrosis by attenuating TGF-β1 signaling, *Lab. Investig.* 98 (8) (2018) 999–1013, <https://doi.org/10.1038/s41374-018-0069-9>.
- [9] T. Armenteros, Z. Andreu, R. Hortigüela, D.C. Lie, H. Mira, BMP and WNT signalling cooperate through LEF1 in the neuronal specification of adult hippocampal neural stem and progenitor cells, *Sci. Rep.* 8 (1) (2018) 9241, <https://doi.org/10.1038/s41598-018-27581-0>.
- [10] G. Le Dréau, BuMPing into neurogenesis: how the canonical BMP pathway regulates neural stem cell divisions throughout space and time, *Front. Neurosci.* 15 (2021) 819990, <https://doi.org/10.3389/fnins.2021.819990>.
- [11] D. Zhang, Z. Lu, J. Man, K. Cui, X. Fu, L. Yu, Y. Gao, L. Liao, Q. Xiao, R. Guo, Y. Zhang, Z. Zhang, X. Liu, H. Lu, J. Wang, Wnt-3a alleviates neuroinflammation after ischemic stroke by modulating the responses of microglia/macrophages and astrocytes, *Int. Immunopharmacol.* 75 (2019) 105760, <https://doi.org/10.1016/j.intimp.2019.105760>.
- [12] N.F. Abo El-Magd, H.A. Ebrahim, M. El-Sherbiny, N.H. Eisa, Quinacrine ameliorates cisplatin-induced renal toxicity via modulation of Sirtuin-1 pathway, *Int. J. Mol. Sci.* 22 (19) (2021), <https://doi.org/10.3390/ijms221910660>.
- [13] M. Ahmad, G.M. Abu-Tawel, A.E. Aboshaiqah, J.S. Ajarem, The effects of quinacrine, proguanil, and pentoxyfylline on seizure activity, cognitive deficit, and oxidative stress in rat lithium-pilocarpine model of status epilepticus, *Oxidative Med. Cell. Longev.* 2014 (2014) 630509, <https://doi.org/10.1155/2014/630509>.
- [14] A.K. Al Asmari, K.T. Al Sadoon, A.A. Obaid, D. Yesunayagam, M. Tariq, Protective effect of quinacrine against glycerol-induced acute kidney injury in rats, *BMC Nephrol.* 18 (1) (2017) 41, <https://doi.org/10.1186/s12882-017-0450-8>.
- [15] S.R. Goulding, M. Lévesque, A.M. Sullivan, L.M. Collins, G.W. O'Keeffe, Quinacrine and Niclosamide promote neurite growth in midbrain dopaminergic neurons through the canonical BMP-Smad pathway and protect against neurotoxin and α-Synuclein-induced neurodegeneration, *Mol. Neurobiol.* 58 (7) (2021) 3405–3416, <https://doi.org/10.1007/s12035-021-02351-8>.
- [16] R.F. Butterworth, M.D. Norenberg, V. Felipo, P. Ferenci, J. Albrecht, A.T. Blei, Experimental models of hepatic encephalopathy: ISHEN guidelines, *Liver Int.* 29 (6) (2009) 783–788, <https://doi.org/10.1111/j.1478-3231.2009.02034.x>.
- [17] C. Kencebay, N. Derin, O. Ozsoy, D. Kipmen-Korgun, G. Tanrıver, N. Ozturk, G. Basaranlar, P. Yargicoglu-Akkiraz, B. Sozen, A. Agar, Merit of quinacrine in the decrease of ingested sulfite-induced toxic action in rat brain, *Food Chem. Toxicol.* 52 (2013) 129–136, <https://doi.org/10.1016/j.fct.2012.11.015>.
- [18] Khader, A. A., Sulaiman, M. A., Kishore, P. N., Morais, C., & Tariq, M. (1996). QUINACRINE ATTENUATES CYCLOSPORINE-INDUCED NEPHROTOXICITY IN RATS. *62(4)*, 427-435. [https://journals.lww.com/transplantjournal/Fulltext/1996/08270/QUINACRINE\\_ATTENUATES\\_CYCLOSPORINE\\_INDUCED\\_1.aspx](https://journals.lww.com/transplantjournal/Fulltext/1996/08270/QUINACRINE_ATTENUATES_CYCLOSPORINE_INDUCED_1.aspx).
- [19] A.M. Fayed, D.F. Mansour, D.O.J.J. Saleh, o. A. P. S., Progression of hepatic encephalopathy induced by bile duct ligation versus thioacetamide in rats: Regulatory role of apigenin, *11 (12)* (2021) 158–168.
- [20] M.H. Sharawy, N. Abdel-Rahman, N. Megahed, M.S. El-Awady, Paclitaxel alleviates liver fibrosis induced by bile duct ligation in rats: role of TGF-β1, IL-10 and c-Myc, *Life Sci.* 211 (2018) 245–251, <https://doi.org/10.1016/j.lfs.2018.09.037>.
- [21] C.G. Tag, S. Sauer-Lehnen, S. Weiskirchen, E. Borkham-Kamphorst, R.H. Tolba, F. Tacke, R. Weiskirchen, Bile duct ligation in mice: induction of inflammatory liver injury and fibrosis by obstructive cholestasis, *J Vis Exp*(96). (2015), <https://doi.org/10.3791/52438>.
- [22] I. Aghaei, M. Nazeri, M. Shabani, M. Mossavinasab, F.K. Mirhosseini, M. Nayebpour, A. Dalili, Erythropoietin ameliorates the motor and cognitive function impairments in a rat model of hepatic cirrhosis, *Metab. Brain Dis.* 30 (1) (2015) 197–204, <https://doi.org/10.1007/s11011-014-9600-x>.
- [23] R.E. Kamal, E. Menze, A. Albohy, H.I. Ahmed, S.S. Azab, Neuroprotective repositioning and anti-tau effect of carvedilol on rotenone induced neurotoxicity in rats: insights from an insilico& in vivo anti-Parkinson's disease study, *Eur. J. Pharmacol.* 932 (2022) 175204, <https://doi.org/10.1016/j.ejphar.2022.175204>.
- [24] A.E. Ali, H.M. Mahdy, D.M. Elsherbiny, S.S. Azab, Rifampicin ameliorates lithium-pilocarpine-induced seizures, consequent hippocampal damage and memory deficit in rats: impact on oxidative, inflammatory and apoptotic machineries, *Biochem. Pharmacol.* 156 (2018) 431–443, <https://doi.org/10.1016/j.bcp.2018.09.004>.
- [25] S.N. Suganya, T. Sumathi, Effect of rutin against a mitochondrial toxin, 3-nitropropionicacid induced biochemical, behavioral and histological alterations-a pilot study on Huntington's disease model in rats, *Metab. Brain Dis.* 32 (2) (2017) 471–481, <https://doi.org/10.1007/s11011-016-9929-4>.
- [26] M. Antunes, G. Biala, The novel object recognition memory: neurobiology, test procedure, and its modifications, *Cogn. Process.* 13 (2) (2012) 93–110, <https://doi.org/10.1007/s10339-011-0430-z>.
- [27] G. Gallo-Oller, R. Ordoñez, J. Dotor, A new background subtraction method for Western blot densitometry band quantification through image analysis software, *J. Immunol. Methods* 457 (2018) 1–5, <https://doi.org/10.1016/j.jim.2018.03.004>.
- [28] C.F.A. Culling, *Handbook of Histopathological and Histochemical Techniques: Including Museum Techniques*, Butterworth-Heinemann, 2013.
- [29] M.Z. Mohamed, M.F. Abed El Baky, M.E. Ali, H.M. Hafez, Aprepitant exerts anti-fibrotic effect via inhibition of TGF-β1/Smad3 pathway in bleomycin-induced pulmonary fibrosis in rats, *Environ. Toxicol. Pharmacol.* 95 (2022) 103940, <https://doi.org/10.1016/j.etap.2022.103940>.
- [30] S. Nardelli, S. Gioia, J. Faccioli, O. Riggio, L. Ridola, Hepatic encephalopathy - recent advances in treatment and diagnosis, *Expert Rev. Gastroenterol. Hepatol.* 17 (3) (2023) 225–235, <https://doi.org/10.1080/17474124.2023.2183386>.
- [31] D. Simicic, C. Cudalbu, K. Pierzchala, Overview of oxidative stress findings in hepatic encephalopathy: from cellular and ammonium-based animal models to human data, *Anal. Biochem.* 654 (2022) 114795, <https://doi.org/10.1016/j.ab.2022.114795>.
- [32] X. Chen, N. Yao, Y. Mao, D. Xiao, Y. Huang, X. Zhang, Y. Wang, Activation of the Wnt/β-catenin/CYP1B1 pathway alleviates oxidative stress and protects the blood-brain barrier under cerebral ischemia/reperfusion conditions, *Neural Regen. Res.* 19 (7) (2024) 1541–1547, <https://doi.org/10.4103/1673-5374.386398>.
- [33] R.L. Huang, Y. Yuan, G.M. Zou, G. Liu, J. Tu, Q. Li, LPS-stimulated inflammatory environment inhibits BMP-2-induced osteoblastic differentiation through crosstalk between TLR4/MyD88/NF-κB and BMP/Smad signaling, *Stem Cells Dev.* 23 (3) (2014) 277–289, <https://doi.org/10.1089/scd.2013.0345>.
- [34] A. González Padrón, E.G. de Toranzo, J.A. Castro, Late preventive effects of quinacrine on carbon tetrachloride induced liver necrosis, *Arch. Toxicol.* 67 (6) (1993) 386–391, <https://doi.org/10.1007/bf01977399>.
- [35] M. Quinn, M. McMillin, C. Galindo, G. Frampton, H.Y. Pae, S. DeMorrow, Bile acids permeabilize the blood brain barrier after bile duct ligation in rats via Rac1-dependent mechanisms, *Dig. Liver Dis.* 46 (6) (2014) 527–534, <https://doi.org/10.1016/j.dld.2014.01.159>.
- [36] M. McMillin, G. Frampton, M. Quinn, S. Ashfaq, de los Santos, M., 3rd, Grant, S., & DeMorrow, S., Bile acid signaling is involved in the neurological decline in a murine model of acute liver failure, *Am. J. Pathol.* 186 (2) (2016) 312–323, <https://doi.org/10.1016/j.ajpath.2015.10.005>.
- [37] L. Dong, X. Han, X. Tao, L. Xu, Y. Xu, L. Fang, L. Yin, Y. Qi, H. Li, J. Peng, Protection by The Total flavonoids from Rosa laevigata Michx fruit against lipopolysaccharide-induced liver injury in mice via modulation of FXR signaling, *Foods* 7 (6) (2018), <https://doi.org/10.3390/foods7060088>.

- [38] Z. Chen, J. Ruan, D. Li, M. Wang, Z. Han, W. Qiu, G. Wu, The role of intestinal Bacteria and gut-brain Axis in hepatic encephalopathy, *Front. Cell. Infect. Microbiol.* 10 (2020) 595759, <https://doi.org/10.3389/fcimb.2020.595759>.
- [39] S.S. Zhao, N.R. Li, W.L. Zhao, H. Liu, M.X. Ge, Y.X. Zhang, L.Y. Zhao, X.F. You, H. W. He, R.G. Shao, D-chiro-inositol effectively attenuates cholestasis in bile duct ligated rats by improving bile acid secretion and attenuating oxidative stress, *Acta Pharmacol. Sin.* 39 (2) (2018) 213–221, <https://doi.org/10.1038/aps.2017.98>.
- [40] F.J. Padillo, A. Cruz, C. Navarrete, I. Bujalance, J. Briceño, J.I. Gallardo, T. Marchal, R. Caballero, I. Túnez, J. Muntané, P. Montilla, C. Pera-Madrazo, Melatonin prevents oxidative stress and hepatocyte cell death induced by experimental cholestasis, *Free Radic. Res.* 38 (7) (2004) 697–704, <https://doi.org/10.1080/10715760410001705131>.
- [41] L. Zhang, Y. Cheng, X. Du, S. Chen, X. Feng, Y. Gao, S. Li, L. Liu, M. Yang, L. Chen, Z. Peng, Y. Yang, W. Luo, R. Wang, W. Chen, J. Chai, Swertiajlanarin, an herbal agent derived from *Swertia mussotii* Franch, attenuates liver injury, inflammation, and cholestasis in common bile duct-ligated rats, *Evid. Based Complement. Alternat. Med.* 2015 (2015) 948376, <https://doi.org/10.1155/2015/948376>.
- [42] M. Harada, K. Morimoto, T. Kondo, R. Hiramatsu, Y. Okina, R. Muko, I. Matsuda, T. Kataoka, Quinacrine inhibits ICAM-1 transcription by blocking DNA binding of the NF- $\kappa$ B subunit p65 and sensitizes human lung adenocarcinoma A549 cells to TNF- $\alpha$  and the Fas ligand, *Int. J. Mol. Sci.* 18 (12) (2017), <https://doi.org/10.3390/ijms18122603>.
- [43] A. Verkhratsky, M. Nedergaard, Physiology of Astroglia, *Physiol. Rev.* 98 (1) (2018) 239–389, <https://doi.org/10.1152/physrev.00042.2016>.
- [44] C.F. Rose, A. Verkhratsky, V. Parpura, Astrocyte glutamine synthetase: pivotal in health and disease, *Biochem. Soc. Trans.* 41 (6) (2013) 1518–1524, <https://doi.org/10.1042/bst20130237>.
- [45] A. Sepehrnejad, A. Zarifkar, G. Namvar, A. Shahbazi, R. Williams, Astrocyte swelling in hepatic encephalopathy: molecular perspective of cytotoxic edema, *Metab. Brain Dis.* 35 (4) (2020) 559–578, <https://doi.org/10.1007/s11011-020-00549-8>.
- [46] C. Stevens, G. Halliday, The role of astrocytes in Parkinson's disease, in: *Inflammation in Parkinson's Disease: Scientific and Clinical Aspects*, Springer, 2014, pp. 127–144.
- [47] D.M.A. Elsherbini, F.M. Ghoneim, E.M. El-Mancy, H.A. Ebrahim, M. El-Sherbiny, M. El-Shafey, R.H. Al-Serwi, N.M. Elsherbiny, Astrocytes profiling in acute hepatic encephalopathy: possible enrolling of glial fibrillary acidic protein, tumor necrosis factor-alpha, inwardly rectifying potassium channel (Kir 4.1) and aquaporin-4 in rat cerebral cortex, *Front. Cell. Neurosci.* 16 (2022) 896172, <https://doi.org/10.3389/fncel.2022.896172>.
- [48] A.R. Jayakumar, X.Y. Tong, J. Ospel, M.D. Norenberg, Role of cerebral endothelial cells in the astrocyte swelling and brain edema associated with acute hepatic encephalopathy, *Neuroscience* 218 (2012) 305–316, <https://doi.org/10.1016/j.neuroscience.2012.05.006>.
- [49] W.Y. Ong, M.L. Go, D.Y. Wang, I.K. Cheah, B. Halliwell, Effects of antimalarial drugs on Neuroinflammation-potential use for treatment of COVID-19-related neurologic complications, *Mol. Neurobiol.* 58 (1) (2021) 106–117, <https://doi.org/10.1007/s12035-020-02093-z>.
- [50] B. Dewidar, C. Meyer, S. Dooley, A.N. Meindl-Beinker, TGF- $\beta$  in hepatic stellate cell activation and liver Fibrogenesis-updated 2019, *Cells* 8 (11) (2019), <https://doi.org/10.3390/cells8111419>.
- [51] Y.L. Yang, H.Z. Ju, S.F. Liu, T.C. Lee, Y.W. Shih, L.Y. Chuang, J.Y. Guh, Y.Y. Yang, T.N. Liao, T.J. Hung, M.Y. Hung, BMP-2 suppresses renal interstitial fibrosis by regulating epithelial-mesenchymal transition, *J. Cell. Biochem.* 112 (9) (2011) 2558–2565, <https://doi.org/10.1002/jcb.23180>.
- [52] Y.L. Yang, Y.S. Liu, L.Y. Chuang, J.Y. Guh, T.C. Lee, T.N. Liao, M.Y. Hung, T. A. Chiang, Bone morphogenetic protein-2 antagonizes renal interstitial fibrosis by promoting catabolism of type I transforming growth factor-beta receptors, *Endocrinology* 150 (2) (2009) 727–740, <https://doi.org/10.1210/en.2008-0090>.
- [53] I. Nakamura, F.Z. Asumda, C.D. Moser, Y.N.N. Kang, J.P. Lai, L.R. Roberts, Sulfatase-2 regulates liver fibrosis through the TGF- $\beta$  signaling pathway, *Cancers (Basel)* 13 (21) (2021), <https://doi.org/10.3390/cancers13215279>.
- [54] M. Yang, C.J.G.H.O.A. Zhang, The role of bone morphogenetic proteins in liver fibrosis, *12* (2021) 17–20.
- [55] F. Wei, Y. Zhou, J. Wang, C. Liu, Y. Xiao, The immunomodulatory role of BMP-2 on macrophages to accelerate osteogenesis, *Tissue Eng. Part A* 24 (7–8) (2018) 584–594, <https://doi.org/10.1089/ten.TEA.2017.0232>.
- [56] M. Alonso, M.R. Viana, A.M. Depino, Mello e Souza, T., Pereira, P., Szapiro, G., Viola, H., Pitossi, F., Izquierdo, I., & Medina, J.H., BDNF-triggered events in the rat hippocampus are required for both short- and long-term memory formation, *Hippocampus* 12 (4) (2002) 551–560, <https://doi.org/10.1002/hipo.10035>.
- [57] K. Yamada, T. Nabeshima, Brain-derived neurotrophic factor/TrkB signaling in memory processes, *J. Pharmacol. Sci.* 91 (4) (2003) 267–270, <https://doi.org/10.1254/jphs.91.267>.
- [58] F. Galland, E. Negri, C. Da Ré, F. Fróes, L. Strapazzon, M.C. Guerra, L.S. Tortorelli, C.A. Gonçalves, M.C. Leite, Hyperammonemia compromises glutamate metabolism and reduces BDNF in the rat hippocampus, *Neurotoxicology* 62 (2017) 46–55, <https://doi.org/10.1016/j.neuro.2017.05.006>.
- [59] E. Gratacós, N. Checa, E. Pérez-Navarro, J. Alberch, Brain-derived neurotrophic factor (BDNF) mediates bone morphogenetic protein-2 (BMP-2) effects on cultured striatal neurones, *J. Neurochem.* 79 (4) (2001) 747–755, <https://doi.org/10.1046/j.1471-4159.2001.00570.x>.
- [60] M. Javadi-Paydar, B. Ghiassy, S. Ebadian, N. Rahimi, A. Norouzi, A.R. Dehpour, Nitric oxide mediates the beneficial effect of chronic naltrexone on cholestasis-induced memory impairment in male rats, *Behav. Pharmacol.* 24 (3) (2013) 195–206, <https://doi.org/10.1097/FBP.0b013e3283618a8c>.
- [61] L. Jafaripour, K. Esmaeilpour, M. Maneshian, H. Bashiri, M.A. Rajizadeh, H. Ahmadvand, M. Asadi-Shekaari, The effect of gallit acid on memory and anxiety-like behaviors in rats with bile duct ligation-induced hepatic encephalopathy: role of AMPK pathway, *Avicenna J Phytomed* 12 (4) (2022) 425–438, <https://doi.org/10.22038/ajp.2022.19720>.
- [62] I. Cho, B.N. Koo, E.H. Kam, S.K. Lee, H. Oh, S.Y. Kim, Bile duct ligation of C57BL/6 mice as a model of hepatic encephalopathy, *Anesth Pain Med (Seoul)* 15 (1) (2020) 19–27, <https://doi.org/10.17085/apm.2020.15.1.19>.
- [63] T. Eshraghi, A. Eidi, P. Mortazavi, A. Asghari, S.M. Tavangar, Magnesium protects against bile duct ligation-induced liver injury in male Wistar rats, *Magnes. Res.* 28 (1) (2015) 32–45, <https://doi.org/10.1684/mrh.2015.0380>.